Computers and Concrete, *Vol. 24, No. 4 (2019) 347-367*
DOI: https://doi.org/10.12989/cac.2019.24.4.347

Influences of porosity on dynamic response of FG plates resting on Winkler/Pasternak/Kerr foundation using quasi 3D HSDT

Farouk Yahia Addou[1], Mustapha Meradjah[2], Abdelmoumen Anis Bousahla[3,4], Abdelkader Benachour[1], Fouad Bourada[1,5], Abdelouahed Tounsi*[1,6] and S.R. Mahmoud[7]

[1]Material and Hydrology Laboratory, Faculty of Technology, Civil Engineering Department, University of Sidi Bel Abbes, Algeria
[2]Civil Engineering Department, Faculty of Technology, University of Sidi Bel Abbes, Algeria
[3]Laboratoire de Modélisation et Simulation Multi-échelle, Université de Sidi Bel Abbés, Algeria
[4]Centre Universitaire de Relizane, Algeria
[5]Département des Sciences et de la Technologie, Centre Universitaire de Tissemsilt, BP 38004 Ben Hamouda, Algeria
[6]Department of Civil and Environmental Engineering, King Fahd University of Petroleum & Minerals, 31261 Dhahran, Eastern Province, Saudi Arabia
[7]GRC Department, Jeddah Community College, King Abdulaziz University, Jeddah, Saudi Arabia

(*Received July 21, 2019, Revised September 3, 2019, Accepted September 11, 2019*)

Abstract. This work investigates the effect of Winkler/Pasternak/Kerr foundation and porosity on dynamic behavior of FG plates using a simple quasi-3D hyperbolic theory. Four different patterns of porosity variations are considered in this study. The used quasi-3D hyperbolic theory is simple and easy to apply because it considers only four-unknown variables to determine the four coupled vibration responses (axial-shear-flexion-stretching). A detailed parametric study is established to evaluate the influences of gradient index, porosity parameter, stiffness of foundation parameters, mode numbers, and geometry on the natural frequencies of imperfect FG plates.

Keywords: Kerr foundation; porous FGM; quasi-3D plate model; vibration

1. Introduction

Functionally graded materials (FGM) were presented in the mid-1980s to be employed as thermal barrier materials against high temperatures. FGMs are advanced materials made of different constituent materials, such as metals, ceramics or polymers, with variable properties in a given spatial direction. This makes it possible to customize the morphologies and the structured characteristics in this specific spatial direction, which improves the mechanical behavior of these materials in terms of stiffness, toughness, hardness, thermal conductivity and corrosion resistance (Sofiyev and Avcar 2010, Bessaim 2013, Naebe and Shirvanimoghaddam 2016, Ebrahimi *et al*. 2017, Zidi *et al*. 2017, El-Haina *et al*. 2017, Avcar and Mohammed 2018, Zarga *et al*. 2019, Karami *et al*. 2019a, b, Hellal *et al*. 2019). In recent years, the trend to use FG plates for use in modern structures has grown considerably. There are many uses of FG structures in the fields of energy conversion, nuclear power engineering, commodities, civil engineering and aerospace. As a result, advances in numerical analysis of FG structures have attracted a lot of attention. One of the most cost-effective ways to advance in numerical investigation is the development of accurate structural models via refined shear deformation theories.

In recent years, extensive studies on FG plates have been performed using conventional plate theory (CPT) and first order shear deformation plate theory (FSDT). Despite its simplicity, the CPT ignores shear deformations and rotational inertia, resulting in less accurate results for thick and moderately thick structures. The FSDT considers transverse shear influences via a shear correction factor and is therefore suitable for the investigation of both thin and moderately thick structures (Al-Basyouni *et al*. 2015, Bouderba *et al*. 2016, Avcar 2016, Youcef *et al*. 2018, Draoui *et al*. 2019). However, the appropriate value of the shear correction coefficient depends on the variation of the Poisson's ratio depending on plate thickness, geometry, load and boundary conditions. Higher order shear deformation theories (HSDTs) do not require a shear correction coefficient and offer the reliable accuracy against to CPT and FSDT. However, these theories lead to a large number of equilibrium equations, greatly increasing the complexity of the problem. As a result, simple theories with fewer unknowns are very attractive. In order to decrease the number of variables employed in the equations of motion, and to satisfy shear deformation influences on the lower and upper faces of the structures without using shear correction factor, Shimpi and Patel (2006a) proposed a refined theory with only two unknown variables for the study of isotropic plates, known as refined plate theory (RPT). Then, different validity studies were carried out on the basis of the RPT. These include the study of isotropic (Shimpi and Patel 2006a, Shahsavari and Janghorban 2017), orthotropic (Shimpi and Patel 2006b), FGM (Karami *et al*. 2018a, Zidi *et al*. 2014) and stratified composite plates (Thai and Kim

*Corresponding author, Professor
E-mail: tou_abdel@yahoo.com

http://www.techno-press.org/?journal=cac&subpage=8
ISSN: 1598-8198 (Print), 1598-818X (Online)

2012). However, until now, various RPT models under the effect of different shape functions by dividing the transverse displacement into bending and shearing parts have been proposed for the study of dynamic (Chaabane *et al*. 2019, Zaoui *et al*. 2019, Bourada *et al*. 2019, Abdelaziz *et al*. 2017, Mouffoki *et al*. 2017, Houari *et al*. 2016, Bellifa *et al*.2016, Attia *et al*. 2015, Karama *et al*. 1998), bending (Hamidi *et al*. 2015, Beldjelili *et al*. 2016, Shahsavari and Janghorban 2017, Abdelaziz *et al*. 2017, Hachemi *et al*. 2017, Kar *et al*. 2017, Bakhadda *et al*. 2018, Attia *et al*. 2018, Younsi *et al*. 2018, Boussoula *et al*. 2019, Meksi *et al*. 2019), wave propagation (Boukhari *et al*. 2016, Benadouda *et al*. 2017, Selmi and Bisharat 2018, Karami *et al*. 2018b, Fourn *et al*. 2018) and buckling (Karama *et al*. 1998, Meziane *et al*. 2014, Bousahla *et al*. 2016, Bouderba *et al*. 2016, Sekkal *et al*. 2017ab, Chikh *et al*. 2017, Menasria *et al*. 2017, Bellifa *et al*. 2017a, b, Tounsi *et al*. 2019) responses of micro and nano-plate structure. Yahia *et al*. (2015) examined the wave behavior of FG plates using RPT with 4-variables in terms of cubic, sinusoidal, hyperbolic, and exponential shear strain shape functions. A refined theory of trigonometric shear deformation (RTSDT) was employed for the thermoelastic bending response of sandwich plates made of FGM by Tounsi *et al*. (2013). Recently, the 4-unknown RPT model using polynomial, exponential and hyperbolic functions is applied to research on shear buckling behavior of nano-plates in a hygro-thermal environment based on the non-local stress gradient theory of Shahsavari *et al*. (2018a).

Often, conventional continuum theories (CPT, FSDT, and HSDTs) neglect the stretching effect of thickness (i.e,, ε_z=0) because of the assumption of constant transverse displacements in the thickness. Recently, the effect of thickness stretching (ε_z) in FG plates using finite element approximations was investigated by Carrera *et al*. (2011) to reach accurate results. Recently, the influence of thickness stretching in FG plates using finite element approximations has been studied by Carrera *et al*. (2011) to obtain accurate results. The thickness stretching influence becomes very valuable for the analysis of thick plates and must therefore be taken into account. On the joint consideration of shear deformation and thickness stretching effects, the many quasi 3D theories, based on higher-order distributions within the thickness for deflections, have been proposed (Thai and Kim 2015). Thai and Kim (2013) have proposed a simple quasi-3D sinusoidal shear-deformation model to study the flexural behavior of FG plates using five unknown variables. Hebali *et al*. (2014) developed a novel quasi-3D model for the analysis of the bending and dynamic of FG plates. An efficient quasi-3D theory has been proposed for FG plates, by dividing the deflection into flexural, shear and stretching components by Belabed *et al*. (2014). Bousahla *et al*. (2014) presented a new quasi-3D theory based on neutral surface position for static study of advanced composite plates. Bourada *et al*. (2015) developed a simple higher-order shear and normal deformation model for FGM beams. Draiche *et al*. (2016) proposed a quasi-3D shear-deformation model for “laminated composite plates”. Thai *et al*. (2014) developed a quasi-3D theory for FG plates by considering a hyperbolic shape function as well as five variables. A sandwich with FGM core and FGM face sheet as well as a sandwich with FGM core and homogeneous face sheet was examined by a new quasi-3D plate model by Bennoun *et al*. (2016).

During the process of manufacturing FGMs, micro-voids are generated during sintering because of the difference in solidification temperature of the constituents of the material (Zhu *et al*. 2001, Li *et al*. 2003). Micro-void formation sources (known as porosity) include air bubbles entering the matrix during melting or mixing processes and formation of water vapor on the surface of the particles in the process of solidification (Aqida *et al*. 2004). Because of the importance of this topic, several works have been conducted to explore the effects of porosity. For example, Yahia *et al*. (2015) investigated the wave propagation in FG plates with porosities using various HSDTs. A HSDT was employed for the study on dynamic of beams made of porous graded materials by Ait Atmane *et al*. (2015). Gupta and Talha (2017) examined the influence of porosity on free vibration behavior of FG plates in the presence of a thermal influence using a non-polynomial quasi 3D HSDT. Benferhat *et al*. (2016a) analyzed the bending response of FG plate with porosities. Also, Benferhat *et al*. (2016b) studied the effect of porosity on the bending and free vibration response of FG plates resting on Winkler-Pasternak foundations. Benadouda *et al*. (2017) studied the effect of porosities on wave propagation in FG beams using an efficient shear deformation theory. Rad *et al*. (2017) analyzed the static response of non-uniform heterogeneous circular plate with porous material resting on a gradient hybrid foundation involving friction force. Akbaş (2017) presented vibration and static analysis of functionally graded porous plates. Eltaher *et al*. (2018) presented a modified porosity model in analysis of FG porous nano-beams. Shahsavari *et al*. (2018b) studied the effect of porosities on free vibration of FG plates resting on elastic foundation. Faleh *et al*. (2018) discussed the vibration properties of porous FG nanoshells. Akbaş (2018) studied the forced vibration behavior of FG porous deep beams. Karami *et al*. (2018c) investigated the thermal buckling of smart porous FG nanobeam rested on Kerr foundation. Avcar (2019) examined the dynamic response of imperfect sigmoid and power law functionally graded beams. Arshid *et al*. (2019) studied the effect of porosity on free vibration of SPFG circular plates resting on visco-Pasternak elastic foundation. Batou *et al*. (2019) studied the wave dispersion properties in imperfect sigmoid plates using various HSDTs.

In recent years, the study of integrated structures in foundations has attracted a lot of attention. To define the interaction between plate and foundation, various assumptions of foundation models have been proposed (Wang*et al*. 2005). The simplest and oldest assumption of the elastic medium models, which has only one substrate reaction coefficient, is known as the Winkler elastic foundation (Winkler 1867). Despite the ease of implementation, the Winkler model is unable to provide continuity in the foundation because of separate springs (Kolahchi *et al*. 2016). This assumption has been improved by the Pasternak model (Pasternak 1954) by adding a shear layer above the springs. The Pasternak model comprising a two-parameter substrate (spring and shear layer) is widely employed to explain the mechanical interactions of flexible plates with different distributions of material properties (Akhavan *et al*. 2009, Hsu 2010, Baferani *et al*. 2011, Lü *et al*. 2009, Bouderba *et al*. 2013, Bounouara *et al*. 2016, Sobhy 2013). In the Kerr Foundation (Kneifati 1985), there are no unconcentrated reactions because of an upper spring layer. This means that, in Kerr's model, a shear layer is surrounded by upper and lower spring layers.

In this work, we examine effects of Winkler/Pasternak/Kerr foundation and porosity on dynamic behavior of imperfect FG plates. For this end, a simple quasi-3D hyperbolic shear deformation plate theory is employed with considering the axial, bending, shear, and thickness stretching effects. Four different patterns of porosity variations are considered for describing porosity influence in graded material characteristics. The Kerr foundation is utilized to describe elastic foundation. The proposed model for the FG plates incorporated into the Kerr foundation will provide the best explanation of the embedded plates compared to that of the Winkler and Pasternak foundations.

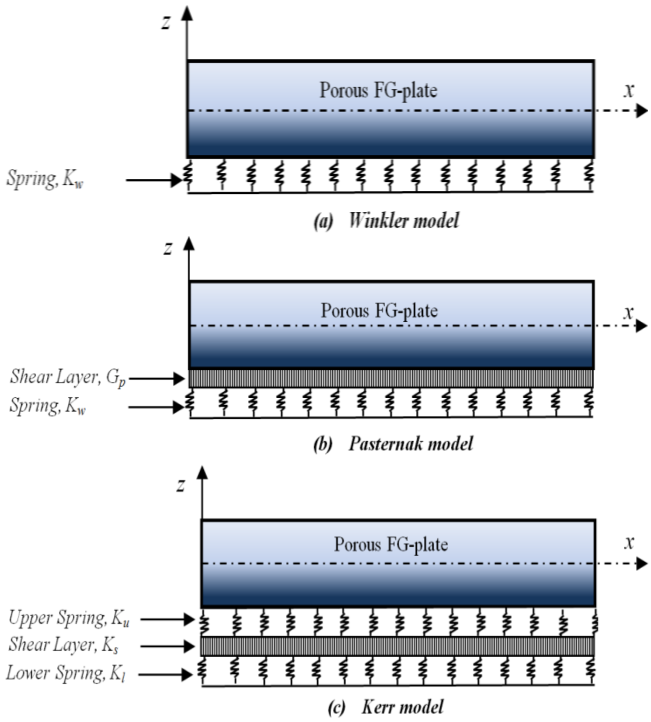

Fig. 1 FG-plates resting on elastic foundations

2. Theoretical formulations

2.1 geometry and concept of functionally graded plate (P-FGM)

In the present study, consider a functionally graded metal-ceramic plates (P-FGM) of length "*a*", width "*b*" and thickness "*h*" in the reference ($x \times y \times z$), respectively. The material properties of FG-plate such as Young's modulus "$E(z)$", mass density "$\rho(z)$" and Poisson's ratio "$\nu(z)$" are assumed to vary continuously through the thickness according to the power law distribution as (Tounsi *et al*. 2013, Houari *et al*. 2013, Bousahla *et al*. 2014, Bourada *et al*. 2015, Fahsi *et al*. 2017)

$$P(z) = P_m + \left(P_c - P_m\right)\left(\frac{z}{h} + \frac{1}{2}\right)^p \tag{1}$$

Where P_m and P_c are the metal and ceramic materials properties, respectively. p is the material index.

The metal-ceramic FG-plate is supposed resting on elastic foundations (type Winkler, Pasternak and Kerr). The illustrative sketches of the three types of elastic foundations are presented in Fig. 1.

2.2 Porous functionally graded plates

The imperfection in the functionally graded materials can be in the form of the micro voids (porosity) that occur during the manufacturing steps of these materials. The micro voids are due to the difference of solidification temperatures between the two materials that constitute the FGM (Zhu *et al*. 2001). Several formulation models of the distribution of the micro voids in functionally graded structures have been proposed such as even, uneven, and logarithmic-uneven porosities.

2.2.1 FG-plate with even porosities

The first model of the porosity distribution was developed by Wattanasakulpong and Ungbhakorn (2014) where the porosity is constant across the thicknesses of the FG-plate (see Fig. 2(a)). The effective materials properties of the FG-plate obtained by introducing the even porosities can be given as

$$P(z) = P_c\left(\left(\frac{1}{2} + \frac{z}{h}\right)^p - \frac{\xi}{2}\right) + P_m\left(1 - \left(\frac{1}{2} + \frac{z}{h}\right)^p - \frac{\xi}{2}\right) \tag{2}$$

Where ξ is the parameter which takes into account the porosity effect.

By applying the Eq. (2) on the effective properties of the FG-plate. The Young's modulus "$E(z)$", mass density "$\rho(z)$" and Poison's ratio "$\nu(z)$" formulations can be expressed as (Wattanasakulpong and Ungbhakorn 2014)

$$E(z) = \left(E_c - E_m\right)\left(\frac{z}{h} + \frac{1}{2}\right)^p + E_m - \frac{\xi}{2}\left(E_c + E_m\right) \tag{3a}$$

$$\nu(z) = \left(\nu_c - \nu_m\right)\left(\frac{z}{h} + \frac{1}{2}\right)^p + \nu_m - \frac{\xi}{2}\left(\nu_c + \nu_m\right) \tag{3b}$$

$$\rho(z) = \left(\rho_c - \rho_m\right)\left(\frac{z}{h} + \frac{1}{2}\right)^p + \rho_m - \frac{\xi}{2}\left(\rho_c + \rho_m\right) \tag{3c}$$

2.2.2 FG-plate with uneven porosities

The infiltration of the materials in the intermediate zone of the plate is very difficult (which increases the risk of production of micro-voids). On the other hand, the infiltration of the material is easy in the free surfaces (upper and lower surfaces) of the plate (the risk of the production

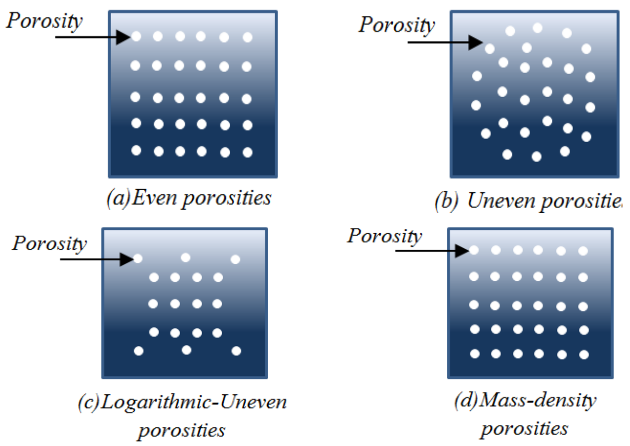

Fig. 2 illustration of different patterns of porosity variations

of the micro voids is low), on the basis of these cases Wattanasakulpong and Ungbhakorn (2014) has developed another model of the porosities distribution (porosity varies across the thickness). The effectives material properties with uneven distribution (see Fig. 2(b)) can be written as

$$E(z)=\left(E_c-E_m\right)\left(\frac{z}{h}+\frac{1}{2}\right)^p+E_m-\frac{\xi}{2}\left(E_c+E_m\right)\left(1-\frac{2|z|}{h}\right) \tag{4a}$$

$$\nu(z)=\left(\nu_c-\nu_m\right)\left(\frac{z}{h}+\frac{1}{2}\right)^p+\nu_m-\frac{\xi}{2}\left(\nu_c+\nu_m\right)\left(1-\frac{2|z|}{h}\right) \tag{4b}$$

$$\rho(z)=\left(\rho_c-\rho_m\right)\left(\frac{z}{h}+\frac{1}{2}\right)^p+\rho_m-\frac{\xi}{2}\left(\rho_c+\rho_m\right)\left(1-\frac{2|z|}{h}\right) \tag{4c}$$

2.2.3 FG-plate with logarithmic-uneven porosities

The third model was proposed by Gupta and Talha (2018) where the distribution of the porosity is varying according to a logarithmic function through the thickness of the plate (see Fig. 2(c)). The effective material properties with logarithmic-uneven distribution can be given as

$$E(z)=\left(E_c-E_m\right)\left(\frac{z}{h}+\frac{1}{2}\right)^p+E_m-\log\left(1+\frac{\xi}{2}\right)\left(E_c+E_m\right)\left(1-\frac{2|z|}{h}\right) \tag{5a}$$

$$\nu(z)=\left(\nu_c-\nu_m\right)\left(\frac{z}{h}+\frac{1}{2}\right)^p+\nu_m-\log\left(1+\frac{\xi}{2}\right)\left(\nu_c+\nu_m\right)\left(1-\frac{2|z|}{h}\right) \tag{5b}$$

$$\rho(z)=\left(\rho_c-\rho_m\right)\left(\frac{z}{h}+\frac{1}{2}\right)^p+\rho_m-\log\left(1+\frac{\xi}{2}\right)\left(\rho_c+\rho_m\right)\left(1-\frac{2|z|}{h}\right) \tag{5c}$$

2.2.4 FG-plate with mass-density porosities

In the present investigation, the fourth model of the porosity is based on the true and the apparent mass density. The formulations of the true and the apparent mass density can be written as

$$m_0=\int_h \rho(z)\ dz\ \ at\ \xi=0\ \ and\ \ m=\int_h \rho(z)\ dz\ \ at\ \xi>0 \tag{6}$$

With

$$\rho(z)=\left(\rho_c-\rho_m\right)\left(\frac{z}{h}+\frac{1}{2}\right)^p+\rho_m-\frac{\xi}{2}\left(\rho_c+\rho_m\right) \tag{7}$$

where "m_0" and "m" are the true and the apparent mass density.

By considering that the elasticity modulus depend on the density of the material, the expression of the Young modulus proposed by Eltaher *et al.* (2018) can be given as

$$E(z)=\left(E_c-E_m\right)\left(\frac{z}{h}+\frac{1}{2}\right)^p+E_m-\frac{m_0-m}{m_0}\left(E_c+E_m\right) \tag{8}$$

2.3 Displacement field and strains:

By introducing the stretching effect on the higher order shear deformation theory (Hebali *et al.* 2016, Merdaci *et al.* 2016, Bourada *et al.* 201, 2018, Elmossouess *et al.* 2017, AitSidhoum *et al.* 2017, Besseghier *et al.* 2017) and keeps the same number of unknowns (Four variables) that is reduced compared to conventional quasi-3D theory. The displacement field of the six unknown quasi-3D theory can be given as

$$u(x,y,z)=u_0(x,y)-z\frac{\partial w_0}{\partial x}+f(z)\phi_x(x,y) \tag{9a}$$

$$v(x,y,z)=v_0(x,y)-z\frac{\partial w_0}{\partial y}+f(z)\phi_y(x,y) \tag{9b}$$

$$w(x,y,z)=w_0(x,y)+g(z)\phi_z(x,y) \tag{9c}$$

The present four unknown hyperbolic quasi-3D shear deformation theory is assumed in the following form (Abualnour *et al.* 2018, Benchohra *et al.* 2018, Bouhadra *et al.* 2018, Boukhlif *et al.* 2019, Boulefrakh *et al.* 2019, Bouanati *et al.* 2019, Khiloun *et al.* 2019, Bendaho *et al.* 2019)

$$u(x,y,z,t)=u_0(x,y,t)-z\frac{\partial w_0}{\partial x}+k_1\ f(z)\int\theta(x,y,t)dx \tag{10a}$$

$$v(x,y,z,t)=v_0(x,y,t)-z\frac{\partial w_0}{\partial y}+k_2\ f(z)\int\theta(x,y,t)dy \tag{10b}$$

$$w(x,y,z,t)=w_0(x,y,t)+g(z)\ \theta(x,y,t) \tag{10c}$$

With

$$f(z)=-\left[\frac{3\pi}{2}z\,\mathrm{sech}^2\left(\frac{1}{2}\right)\right]+\frac{3\pi}{2}h\tanh\left(\frac{z}{h}\right)$$
$$\text{and}\quad g(z)=\frac{2}{15}\frac{\partial f(z)}{\partial z} \tag{11}$$

Where the terms (u_0;v_0;w_0 and θ) are four unknown displacements of the mid-plane of the plate and the coefficient "k_1" and "k_2" depends on the geometry.

Based on the kinematic of Eq. (10), the strain-displacement expressions can be obtained as

$$\begin{Bmatrix} \varepsilon_x \\ \varepsilon_y \\ \gamma_{xy} \end{Bmatrix} = \begin{Bmatrix} \varepsilon_x^0 \\ \varepsilon_y^0 \\ \gamma_{xy}^0 \end{Bmatrix} + z \begin{Bmatrix} k_x^b \\ k_y^b \\ k_{xy}^b \end{Bmatrix} + f(z) \begin{Bmatrix} k_x^s \\ k_y^s \\ k_{xy}^s \end{Bmatrix},$$
$$\begin{Bmatrix} \gamma_{yz} \\ \gamma_{xz} \end{Bmatrix} = f'(z) \begin{Bmatrix} \gamma_{yz}^0 \\ \gamma_{xz}^0 \end{Bmatrix} + g(z) \begin{Bmatrix} \gamma_{yz}^1 \\ \gamma_{xz}^1 \end{Bmatrix}, \quad \varepsilon_z = g'(z)\,\varepsilon_z^0 \tag{12}$$

with

$$\begin{Bmatrix} \varepsilon_x^0 \\ \varepsilon_y^0 \\ \gamma_{xy}^0 \end{Bmatrix} = \begin{Bmatrix} \dfrac{\partial u_0}{\partial x} \\ \dfrac{\partial v_0}{\partial x} \\ \dfrac{\partial u_0}{\partial y} + \dfrac{\partial v_0}{\partial x} \end{Bmatrix}, \quad \begin{Bmatrix} k_x^b \\ k_y^b \\ k_{xy}^b \end{Bmatrix} = \begin{Bmatrix} -\dfrac{\partial^2 w_0}{\partial x^2} \\ -\dfrac{\partial^2 w_0}{\partial y^2} \\ -2\dfrac{\partial^2 w_0}{\partial x \partial y} \end{Bmatrix}, \tag{13a}$$

$$\begin{Bmatrix} k_x^s \\ k_y^s \\ k_{xy}^s \end{Bmatrix} = \begin{Bmatrix} k_1 \theta \\ k_2 \theta \\ k_1 \dfrac{\partial}{\partial y}\displaystyle\int \theta\, dx + k_2 \dfrac{\partial}{\partial x}\displaystyle\int \theta\, dy \end{Bmatrix}$$
$$\begin{Bmatrix} \gamma_{yz}^0 \\ \gamma_{xz}^0 \end{Bmatrix} = \begin{Bmatrix} k_2 \int \theta\, dy \\ k_1 \int \theta\, dx \end{Bmatrix}, \begin{Bmatrix} \gamma_{yz}^1 \\ \gamma_{xz}^1 \end{Bmatrix} = \begin{Bmatrix} \dfrac{\partial \theta}{\partial y} \\ \dfrac{\partial \theta}{\partial x} \end{Bmatrix},$$
$$\varepsilon_z^0 = \theta \quad \text{and} \quad g'(z) = \frac{dg(z)}{dz} \tag{13b}$$

The undetermined integrals $\int \theta\, dx$; $\int \theta\, dy$; $\dfrac{\partial}{\partial y}\int \theta\, dx$; $\dfrac{\partial}{\partial x}\int \theta\, dy$ mentioned in the previous equations shall be resolved via Navier solution and can be obtained as follows

$$\int \theta\, dx = A' \frac{\partial \theta}{\partial x}, \quad \int \theta\, dy = B' \frac{\partial \theta}{\partial y},$$
$$\frac{\partial}{\partial y}\int \theta\, dx = A' \frac{\partial^2 \theta}{\partial x \partial y}, \quad \frac{\partial}{\partial x}\int \theta\, dy = B' \frac{\partial^2 \theta}{\partial x \partial y} \tag{14}$$

where the coefficients "A'" and "B'" are defined according to the type of method used. In this case using Navier solution, the terms A', B', k_1 and k_2 are obtained as follows

$$A' = -\frac{1}{\alpha^2}, \quad B' = -\frac{1}{\beta^2}, k_1 = -\alpha^2, k_2 = -\beta^2 \tag{15}$$

where α and β are defined in expression 41.

For functionally graded material, the linear constitution relations (stress-strain) can be written as

$$\begin{Bmatrix} \sigma_x \\ \sigma_y \\ \sigma_z \\ \tau_{xy} \\ \tau_{xz} \\ \tau_{yz} \end{Bmatrix} = \begin{bmatrix} C_{11} & C_{12} & C_{13} & 0 & 0 & 0 \\ C_{12} & C_{22} & C_{23} & 0 & 0 & 0 \\ C_{13} & C_{23} & C_{33} & 0 & 0 & 0 \\ 0 & 0 & 0 & C_{66} & 0 & 0 \\ 0 & 0 & 0 & 0 & C_{55} & 0 \\ 0 & 0 & 0 & 0 & 0 & C_{44} \end{bmatrix} \begin{Bmatrix} \varepsilon_x \\ \varepsilon_y \\ \varepsilon_z \\ \gamma_{xy} \\ \gamma_{xz} \\ \gamma_{yz} \end{Bmatrix} \tag{16}$$

where "σ and τ" are the normal and shear stresses and "ε and γ" are the strain components. The elastic constants expressions C_{ij} in terms of engineering are given below (Hebali *et al*. 2014, Benahmed *et al*. 2017, Shahsavari *et al*. 2018b, Ait Sidhoum *et al*. 2018):

• If the stretching effect is negligible "ε_z=0", the 2D elastic constants "C_{ij}" can be defined as

$$C_{11} = C_{22} = \frac{E(z)}{(1 - \nu(z)^2)}, \tag{17}$$

$$C_{12} = \frac{\nu E(z)}{(1 - \nu(z)^2)}, \tag{18}$$

$$C_{44} = C_{55} = C_{66} = \frac{E(z)}{2\,(1 + \nu(z))}, \tag{19}$$

• If the stretching effect is considered "$\varepsilon_z \neq 0$", the 3D elastic constants "C_{ij}" can be expressed as

$$C_{11} = C_{22} = C_{33} = \frac{1 - \nu(z)}{\nu(z)} \lambda(z), \tag{20}$$

$$C_{12} = C_{13} = C_{23} = \lambda(z), \tag{21}$$

$$C_{44} = C_{55} = C_{66} = \mu(z), \tag{22}$$

With

$$\lambda(z) = \frac{\nu(z)\, E(z)}{(1 - 2\nu(z))\,(1 + \nu(z))}$$
$$\text{And} \quad \mu(z) = G(z) = \frac{E(z)}{2\,(1 + \nu(z))} \tag{23}$$

where $\mu(z)$ Lamé's coefficients.

2.4 Equations of motion

The equations of motion of the free vibration analysis of simply supported FG-plate resting on elastic foundation can be derived by employing the Hamilton's energy principle (HEP). The analytical form of the principle (HEP) can be expressed as follow (Mahi *et al*. 2015, Bennai *et al*. 2015, Zemri *et al*. 2015)

$$\int_0^t (\delta U + \delta U_F - \delta K)\, dt = 0 \tag{24}$$

where δU, δU_F and δK are the virtual strain energy, the strain energy induced by elastic foundations and the variation of kinetic energy, respectively.

The variation of the virtual strain energy (δU) of the FG-plate can be rewritten as

$$\delta U = \int_V \begin{bmatrix} \sigma_x \delta\, \varepsilon_x + \sigma_y \delta\, \varepsilon_y + \sigma_z \delta\, \varepsilon_z + \tau_{xy} \delta\, \gamma_{xy} + \\ \tau_{yz} \delta\, \gamma_{yz} + \tau_{xz} \delta\, \gamma_{xz} \end{bmatrix} dV$$
$$= \int_\Omega \begin{bmatrix} N_x \delta\, \varepsilon_x^0 + N_y \delta\, \varepsilon_y^0 + N_z \delta\, \varepsilon_z^0 + N_{xy} \delta\, \gamma_{xy}^0 + \\ M_x^b \delta\, k_x^b + M_y^b \delta\, k_y^b + M_{xy}^b \delta\, k_{xy}^b + M_x^s \delta\, k_x^s + \\ M_y^s \delta\, k_y^s + M_{xy}^s \delta\, k_{xy}^s + Q_{yz}^s \delta\, \gamma_{yz}^0 + S_{yz}^s \delta\, \gamma_{yz}^1 + \\ Q_{xz}^s \delta\, \gamma_{xz}^0 + S_{xz}^s \delta\, \gamma_{xz}^1 \end{bmatrix} dA \tag{25}$$

Where A is the top surface and "N,M,S and Q" are the stress resultants, with

$$(N_i, M_i^b, M_i^s) = \int_{-h/2}^{h/2} (1, z, f)\ \sigma_i\ dz, \quad (i = x, y, xy)\ ; \qquad N_z = \int_{-h/2}^{h/2} g'(z)\,\sigma_z\ dz \tag{26a}$$

$$(S_{xz}^s, S_{yz}^s) = \int_{-h/2}^{h/2} g(z)(\tau_{xz}, \tau_{yz})\ dz, \qquad (Q_{xz}^s, Q_{yz}^s) = \int_{-h/2}^{h/2} f'(z)\ (\tau_{xz}, \tau_{yz})\ dz, \tag{26b}$$

The elastic foundation models employed in the present investigation are illustrated in the Fig. 1. The strain energy induced by the elastic foundations (Winkler, Pasternak and Kerr) can be defined as

$$\delta\ U_F = -\int_V \left\{ U_{Winkler} + U_{Pasternak} + U_{Kerr} \right\}\ dV = -(q_{Winkler} + q_{Pasternak} + q_{Kerr}) \tag{27}$$

In the case of the present four unknown's quasi-3D plate theory, the distributed load cited in the Eq. (27) can be defined by:

Winkler model

This model contains a single parameter (which represents independent springs) and can be expressed as

$$q_{Winkler} = K_w w_0 \tag{28}$$

Where K_w is the constant transverse stiffness coefficient of the elastic medium (so-called spring constant).

Pasternak model

This model contains two elastic parameters, the first is the same of the Winkler (springs) and the second is a shear layer parameter (shear action) which depicts the interaction between the spring parts (Shahsavari *et al.* 2018b), and the Pasternak reaction can be defined as

$$q_{Pasternak} = K_w w_0 - G_p \nabla^2 w_0 \tag{29}$$

Where G_p is the shear stiffness and ∇^2 represent the rectangular Cartesian coordinates, the Laplace differential operator is defined as

$$\nabla^2 = \partial^2/\partial x^2 + \partial^2/\partial y^2 \tag{30}$$

To obtain the Winkler foundation model from the Pasternak model just put G_p=0 in Eq. (29).

Kerr model

This model is composed of three elastic layers, independent upper and lower layers modeled by springs (with stiffness's K_u and K_l, respectively) and an intermediate shear layer with stiffness K_s (Shahsavari *et al.* 2018b). The distributed reaction of this last model (Kerr foundation) is defined as

$$\left(q_{Kerr} - \left(\frac{K_s K_u}{K_l + K_u} \right) \nabla^2 q_{Kerr} \right) = \left(\frac{K_l K_u}{K_l + K_u} \right) w_0 - \left(\frac{K_s K_u}{K_l + K_u} \right) \nabla^2 w_0 \tag{31}$$

This type of Kerr foundation is taken into account for the first time for the present displacement field of quasi-3D plate theories with only four unknowns.

The expression of the variation of kinetic energy of the FG-plate can be written as (Belkorissat *et al.* 2015, Larbi Chaht *et al.* 2015, Belabed *et al.* 2018, Bouafia *et al.* 2018)

$$\begin{aligned}
\delta\ K &= \int_V \left[\dot{u}\,\delta\ \dot{u} + \dot{v}\,\delta\ \dot{v} + \dot{w}\,\delta\ \dot{w} \right]\ \rho(z)\ dV \\
&= \int_A \Bigg\{ I_0 \left[\dot{u}_0 \delta \dot{u}_0 + \dot{v}_0 \delta \dot{v}_0 + \dot{w}_0 \delta \dot{w}_0 \right] \\
&\quad - I_1 \begin{pmatrix} \dot{u}_0 \dfrac{\partial \delta \dot{w}_0}{\partial x} + \dfrac{\partial \dot{w}_0}{\partial x} \delta\ \dot{u}_0 + \\ \dot{v}_0 \dfrac{\partial \delta \dot{w}_0}{\partial y} + \dfrac{\partial \dot{w}_0}{\partial y} \delta\ \dot{v}_0 \end{pmatrix} \\
&\quad + J_1 \begin{pmatrix} (k_1 A') \left(\dot{u}_0 \dfrac{\partial \delta \dot{\theta}}{\partial x} + \dfrac{\partial \dot{\theta}}{\partial x} \delta\ \dot{u}_0 \right) + \\ (k_2 B') \left(\dot{v}_0 \dfrac{\partial \delta \dot{\theta}}{\partial y} + \dfrac{\partial \dot{\theta}}{\partial y} \delta\ \dot{v}_0 \right) + \\ J_1^{st} (\dot{w}_0 \delta \dot{\theta} + \dot{\theta} \delta \dot{w}_0) \end{pmatrix} \\
&\quad + I_2 \left(\frac{\partial \dot{w}_0}{\partial x} \frac{\partial \delta\ \dot{w}_0}{\partial x} + \frac{\partial \dot{w}_0}{\partial y} \frac{\partial \delta\ \dot{w}_0}{\partial y} \right) + \\
&\quad K_2 \left((k_1 A')^2 \left(\frac{\partial \dot{\theta}}{\partial x} \frac{\partial \delta\ \dot{\theta}}{\partial x} \right) + (k_2 B')^2 \left(\frac{\partial \dot{\theta}}{\partial y} \frac{\partial \delta\ \dot{\theta}}{\partial y} \right) \right) \\
&\quad - J_2 \begin{pmatrix} (k_1 A') \left(\dfrac{\partial \dot{w}_0}{\partial x} \dfrac{\partial \delta\ \dot{\theta}}{\partial x} + \dfrac{\partial \dot{\theta}}{\partial x} \dfrac{\partial \delta\ \dot{w}_0}{\partial x} \right) + \\ (k_2 B') \left(\dfrac{\partial \dot{w}_0}{\partial y} \dfrac{\partial \delta\ \dot{\theta}}{\partial y} + \dfrac{\partial \dot{\theta}}{\partial y} \dfrac{\partial \delta\ \dot{w}_0}{\partial y} \right) + \\ K_2^{st}\, \dot{\theta} \delta \dot{\theta} \end{pmatrix} \Bigg\} dA
\end{aligned} \tag{32}$$

where (I_i, J_i and K_i) are mass inertias of the FG-plate and dot-superscript convention indicate the differentiation with respect to the time variable t.

$$(I_0, I_1, I_2) = \int_{-h/2}^{h/2} (1, z, z^2)\,\rho(z)\,dz \tag{33a}$$

$$(J_1, J_1^{st}, J_2, K_2, K_2^{st}) = \int_{-h/2}^{h/2} (f, g, zf, f^2, g^2)\,\rho(z)\,dz \tag{33b}$$

By substituting the virtual strain energy (Eq. (25)), The strain energy induced by elastic foundations (Eq. (27)) and the variation of kinetic energy (Eq. (32)) into expression of

Hamilton energy principle (Eq. (24)), integrating by part and separate the terms of displacement (δu_0; δv_0; δw_0 and $\delta\theta$). The equations of motion can be obtained as follow

$$
\begin{aligned}
&\delta\, u_0: \quad \frac{\partial N_x}{\partial x}+\frac{\partial N_{xy}}{\partial y}=I_0\ddot{u}_0-I_1\frac{\partial \ddot{w}_0}{\partial x}+J_1k_1A'\frac{\partial\ddot{\theta}}{\partial x}\\
&\delta\, v_0: \quad \frac{\partial N_{xy}}{\partial x}+\frac{\partial N_y}{\partial y}=I_0\ddot{v}_0-I_1\frac{\partial \ddot{w}_0}{\partial y}+J_1k_2B'\frac{\partial\ddot{\theta}}{\partial y}\\
&\delta\, w_0: \quad \frac{\partial^2 M_x^b}{\partial x^2}+2\frac{\partial^2 M_{xy}^b}{\partial x\partial y}+\frac{\partial^2 M_y^b}{\partial y^2}-q_{Winkler}-\\
&\qquad q_{Pasternak}-q_{Kerr}=I_0\ddot{w}_0+I_1\left(\frac{\partial\ddot{u}_0}{\partial x}+\frac{\partial\ddot{v}_0}{\partial y}\right)+\\
&\qquad J_2\left(k_1A'\frac{\partial^2\ddot{\theta}}{\partial x^2}+k_2B'\frac{\partial^2\ddot{\theta}}{\partial y^2}\right)-I_2\nabla^2\ddot{w}_0+J0_1^{st}\ddot{\theta}\\
&\delta\,\theta: \quad -k_1A'\frac{\partial^2 M_x^s}{\partial x^2}-k_2B'\frac{\partial^2 M_y^s}{\partial y^2}-\\
&\qquad \left(k_1A'+k_2B'\right)\frac{\partial^2 M_{xy}^s}{\partial x\partial y}+k_1A'\frac{\partial Q_{xz}}{\partial x}+\\
&\qquad k_2B'\frac{\partial Q_{yz}}{\partial y}-N_z+\frac{\partial S_{xz}^s}{\partial x}+\frac{\partial S_{yz}^s}{\partial y}=\\
&\qquad -J_1\left(k_1A'\frac{\partial\ddot{u}_0}{\partial x}+k_2B'\frac{\partial\ddot{v}_0}{\partial y}\right)+\\
&\qquad J_2\left(k_1A'\frac{\partial^2\ddot{w}_0}{\partial x^2}+k_2B'\frac{\partial^2\ddot{w}_0}{\partial y^2}\right)\\
&\qquad -K_2\left((k_1A')^2\frac{\partial^2\ddot{\theta}}{\partial x^2}+(k_2B')^2\frac{\partial^2\ddot{\theta}}{\partial y^2}\right)+J_1^{st}\ddot{w}_0+K_2^{st}\ddot{\theta}
\end{aligned}
\tag{34}
$$

Substituting Eq. (12) into Eq. (16) and the obtained results into Eq. (26), the stress resultants N,M,Q and S are obtained in terms of strains ε, k^b, k^s and γ as follow

$$
\begin{Bmatrix} N\\ M^b\\ M^s\end{Bmatrix}=\begin{bmatrix} A & B & B^s\\ B & D & D^s\\ B^s & D^s & H^s\end{bmatrix}\begin{Bmatrix}\varepsilon\\ k^b\\ k^s\end{Bmatrix}+\varepsilon^0\begin{Bmatrix} L\\ L^a\\ R\end{Bmatrix},\quad
\begin{Bmatrix} Q\\ S\end{Bmatrix}=\begin{bmatrix} F^s & X^s\\ X^s & A^s\end{bmatrix}\begin{Bmatrix}\gamma^0\\ \gamma^1\end{Bmatrix}
\tag{35a}
$$

$$
N_z=L(\varepsilon_x^0+\varepsilon_y^0)+L^a(k_x^b+k_y^b)+R(k_x^s+k_y^s)+R^a\varepsilon_z^0 \tag{35b}
$$

in which

$$
N=\left\{N_x,N_y,N_{xy}\right\}^t,\ M^b=\left\{M_x^b,M_y^b,M_{xy}^b\right\}^t,\quad M^s=\left\{M_x^s,M_y^s,M_{xy}^s\right\}^t, \tag{36a}
$$

$$
\varepsilon=\left\{\varepsilon_x^0,\varepsilon_y^0,\gamma_{xy}^0\right\}^t,\ k^b=\left\{k_x^b,k_y^b,k_{xy}^b\right\}^t,\quad k^s=\left\{k_x^s,k_y^s,k_{xy}^s\right\}^t, \tag{36b}
$$

$$
A=\begin{bmatrix} A_{11} & A_{12} & 0\\ A_{12} & A_{22} & 0\\ 0 & 0 & A_{66}\end{bmatrix},\quad B=\begin{bmatrix} B_{11} & B_{12} & 0\\ B_{12} & B_{22} & 0\\ 0 & 0 & B_{66}\end{bmatrix},
$$

$$
D=\begin{bmatrix} D_{11} & D_{12} & 0\\ D_{12} & D_{22} & 0\\ 0 & 0 & D_{66}\end{bmatrix}, \tag{36c}
$$

$$
B^s=\begin{bmatrix} B_{11}^s & B_{12}^s & 0\\ B_{12}^s & B_{22}^s & 0\\ 0 & 0 & B_{66}^s\end{bmatrix},\ D^s=\begin{bmatrix} D_{11}^s & D_{12}^s & 0\\ D_{12}^s & D_{22}^s & 0\\ 0 & 0 & D_{66}^s\end{bmatrix},\quad H^s=\begin{bmatrix} H_{11}^s & H_{12}^s & 0\\ H_{12}^s & H_{22}^s & 0\\ 0 & 0 & H_{66}^s\end{bmatrix}, \tag{36d}
$$

$$
Q=\left\{Q_{xz}^s,Q_{yz}^s\right\}^t,\ S=\left\{S_{xz}^s,S_{yz}^s\right\}^t,\quad \gamma^0=\left\{\gamma_{xz}^0,\gamma_{yz}^0\right\}^t,\ \gamma^1=\left\{\gamma_{xz}^1,\gamma_{yz}^1\right\}^t \tag{36e}
$$

$$
F^s=\begin{bmatrix} F_{55}^s & 0\\ 0 & F_{44}^s\end{bmatrix},\ X^s=\begin{bmatrix} X_{55}^s & 0\\ 0 & X_{44}^s\end{bmatrix},\quad A^s=\begin{bmatrix} A_{55}^s & 0\\ 0 & A_{44}^s\end{bmatrix} \tag{36f}
$$

$$
\begin{Bmatrix} L\\ L^a\\ R\\ R^a\end{Bmatrix}=\int_z \lambda(z)\begin{Bmatrix} 1\\ z\\ f(z)\\ g'(z)\dfrac{1-\nu(z)}{\nu(z)}\end{Bmatrix}g'(z)dz \tag{36g}
$$

and stiffness components A, B, D, B^s, D^s, H^s, F^s, X^s and A^s are given as

$$
\begin{Bmatrix} A_{11} & B_{11} & D_{11} & B_{11}^s & D_{11}^s & H_{11}^s\\ A_{12} & B_{12} & D_{12} & B_{12}^s & D_{12}^s & H_{12}^s\\ A_{66} & B_{66} & D_{66} & B_{66}^s & D_{66}^s & H_{66}^s\end{Bmatrix}=
\int_z \lambda(z)(1,z,z^2,f(z),zf(z),f^2(z))\begin{Bmatrix}\dfrac{1-\nu(z)}{\nu(z)}\\ 1\\ \dfrac{1-2\nu(z)}{2\nu(z)}\end{Bmatrix}dz \tag{37a}
$$

$$
(A_{22},B_{22},D_{22},B_{22}^s,D_{22}^s,H_{22}^s)=(A_{11},B_{11},D_{11},B_{11}^s,D_{11}^s,H_{11}^s) \tag{37b}
$$

$$
(F_{44}^s,X_{44}^s,A_{44}^s)=\int_{-h/2}^{h/2}\frac{E(z)}{2(1+\nu(z))}\left(\left[f'(z)\right]^2,f'(z)g(z),g^2(z)\right)dz \tag{37c}
$$

$$
(F_{55}^s,X_{55}^s,A_{55}^s)=(F_{44}^s,X_{44}^s,A_{44}^s) \tag{37d}
$$

By substituting Eqs. (35) into Eq. (34), the equation of motion can be expressed in terms of displacements (u_0, v_0, w_0, θ) and the appropriate equations are obtained as

$$\begin{aligned}&A_{11}d_{11}u_0 + A_{66}\,d_{22}u_0 + \left(A_{12}+A_{66}\right)d_{12}v_0 - B_{11}d_{111}w_0\\&-\left(B_{12}+2B_{66}\right)d_{122}w_0 + \left(B_{66}^s\left(k_1A'+k_2\,B'\right)+B_{12}^s k_2B'\right)d_{122}\theta\\&+B_{11}^s k_1A'd_{111}\theta + Ld_1\theta = I_0\ddot{u}_0 - I_1d_1\ddot{w}_0 + J_1k_1A'd_1\ddot{\theta}\end{aligned} \tag{38a}$$

$$\begin{aligned}&A_{22}\,d_{22}v_0 + A_{66}\,d_{11}v_0 + \left(A_{12}+A_{66}\right)d_{12}u_0 - B_{22}\,d_{222}w_0\\&-\left(B_{12}+2B_{66}\right)d_{112}w_0 + \left(B_{66}^s\left(k_1A'+k_2\,B'\right)+B_{12}^s k_1A'\right)d_{112}\theta\\&+B_{22}^s k_2B'd_{222}\theta + Ld_2\theta = I_0\ddot{v}_0 - I_1d_2\ddot{w}_0 + J_1k_2B'd_2\ddot{\theta}\end{aligned} \tag{38b}$$

$$\begin{aligned}&B_{11}\,d_{111}u_0 + \left(B_{12}+2B_{66}\right)d_{122}u_0 + \left(B_{12}+2B_{66}\right)d_{112}v_0\\&+B_{22}\,d_{222}v_0 - D_{11}d_{1111}w_0 - 2\left(D_{12}+2D_{66}\right)d_{1122}w_0\\&-D_{22}\,d_{2222}w_0 + D_{11}^s\,k_1A'\,d_{1111}\theta +\\&\left((D_{12}^s+2D_{66}^s)\left(k_1A'+k_2B'\right)\right)d_{1122}\theta + D_{22}^s k_2B'd_{2222}\theta +\\&L^a(d_{11}\theta + d_{22}\theta) - \left(K_w w_0 - G_p(d_{11}w_0 + d_{22}w_0)\right)\\&-\left(\left(\frac{K_lK_u}{K_l+K_u}\right)w_0 - \left(\frac{K_sK_u}{K_l+K_u}\right)(d_{11}w_0 + d_{22}w_0)\right) = I_0\ddot{w}_0\\&+I_1\left(d_1\ddot{u}_0 + d_2\ddot{v}_0\right) - I_2(d_{11}\ddot{w}_0 + d_{22}\ddot{w}_0)\\&+J_2\left(k_1A'd_{11}\ddot{\theta} + k_2B'd_{22}\ddot{\theta}\right) + J_1^{st}\ddot{\theta}\end{aligned} \tag{38c}$$

$$\begin{aligned}&-k_1A'B_{11}^s d_{111}u_0 - \left(B_{12}^s k_2B' + B_{66}^s\left(k_1A'+k_2B'\right)\right)d_{122}u_0\\&-\left(B_{12}^s k_1A' + B_{66}^s\left(k_1A'+k_2B'\right)\right)d_{112}v_0 - B_{22}^s k_2B'd_{222}v_0\\&+D_{11}^s k_1A'd_{1111}w_0 + \left((D_{12}^s+2D_{66}^s)\left(k_1A'+k_2B'\right)\right)d_{1122}w_0\\&+D_{22}^s k_2B'd_{2222}w_0 - H_{11}^s(k_1A')^2 d_{1111}\theta - H_{22}^s(k_2B')^2 d_{2222}\theta\\&-\left(2H_{12}^s k_1A'k_2B' + \left(k_1A'+k_2B'\right)^2 H_{66}^s\right)d_{1122}\theta\\&+\left((k_1A')^2F_{55}^s + 2k_1A'X_{55}^s + A_{55}^s\right)d_{11}\theta\\&+\left((k_2B')^2F_{44}^s + 2k_2B'X_{44}^s + A_{44}^s\right)d_{22}\theta\\&-2R(k_1A'd_{11}\theta + k_2B'd_{22}\theta) - L(d_1u_0 + d_2v_0)\\&+L^a(d_{11}w_0 + d_{22}w_0) - R^a\theta = -J_1\left(k_1A'd_1\ddot{u}_0 + k_2B'd_2\ddot{v}_0\right)\\&+J_2(k_1A'd_{11}\ddot{w}_0 + k_2B'd_{22}\ddot{w}_0) -\\&K_2\left((k_1A')^2d_{11}\ddot{\theta} + (k_2B')^2d_{22}\ddot{\theta}\right) + J_1^{st}\ddot{w}_0 + K_2^{st}\ddot{\theta}\end{aligned} \tag{38d}$$

Where the following differential operators (d_{ij}, d_{ijl} and d_{ijlm}) are given as

$$d_{ij} = \frac{\partial^2}{\partial x_i \partial x_j},\quad d_{ijl} = \frac{\partial^3}{\partial x_i \partial x_j \partial x_l},\ d_{ijlm} = \frac{\partial^4}{\partial x_i \partial x_j \partial x_l \partial x_m},$$
$$d_i = \frac{\partial}{\partial x_i},\quad (i,j,l,m = 1,2). \tag{39}$$

2.5 Closed-form solutions

In this investigation, Navier solution method is employed to solve the equation of motion of Eq. (38) and assured the boundary conditions (simply supported). The Navier method can be expressed in double trigonometric functions as follow

$$\begin{Bmatrix} u_0\\ v_0\\ w_0\\ \theta \end{Bmatrix} = \sum_{m=1}^{\infty}\sum_{n=1}^{\infty}\begin{Bmatrix} U_{mn}e^{i\omega t}\cos(\alpha\,x)\sin(\beta\,y)\\ V_{mn}e^{i\omega t}\sin(\alpha\,x)\cos(\beta\,y)\\ W_{mn}e^{i\omega t}\sin(\alpha\,x)\sin(\beta\,y)\\ X_{mn}e^{i\omega t}\sin(\alpha\,x)\sin(\beta\,y)\end{Bmatrix} \tag{40}$$

where ω is the frequency of free vibration of the FG-plate, $\sqrt{i} = -1$ the imaginary unit with

$$\alpha = m\pi / a \quad \text{and}\ \beta = n\pi / b \tag{41}$$

Substituting Eq. (40) into Eq. (38), the following equation is obtained

$$\left(\begin{bmatrix} S_{11} & S_{12} & S_{13} & S_{15}\\ S_{12} & S_{22} & S_{23} & S_{24}\\ S_{13} & S_{23} & S_{33} & S_{34}\\ S_{14} & S_{24} & S_{34} & S_{44}\end{bmatrix} - \omega^2\begin{bmatrix} m_{11} & 0 & m_{13} & m_{14}\\ 0 & m_{22} & m_{23} & m_{24}\\ m_{13} & m_{23} & m_{33} & m_{34}\\ m_{14} & m_{24} & m_{34} & m_{44}\end{bmatrix}\right)\begin{Bmatrix} U_{mn}\\ V_{mn}\\ W_{mn}\\ X_{mn}\end{Bmatrix} = \begin{Bmatrix}0\\0\\0\\0\end{Bmatrix} \tag{42}$$

Where

$$\begin{aligned}&S_{11} = (\alpha^2A_{11} + \beta^2A_{66})\\&S_{12} = \alpha\beta(A_{12} + A_{66})\\&S_{13} = -\alpha^3B_{11} - \alpha\beta^2(B_{12} + 2B_{66})\\&S_{14} = \alpha((k_2B'B_{12}^s + (k_1A' + k_2B')B_{66}^s)\beta^2\\&\quad + k_1A'B_{11}^s\alpha^2 - L)\\&S_{22} = (\alpha^2A_{66} + \beta^2A_{22})\\&S_{23} = -\alpha^2\beta(B_{12} + 2B_{66}) - \beta^3B_{22}\\&S_{24} = \beta((k_1A'B_{12}^s + (k_1A' + k_2B')B_{66}^s)\alpha^2 +\\&\quad k_2B'B_{22}^s\beta^2 - L)\\&S_{33} = (\alpha^4D_{11} + \beta^4D_{22} + 2\alpha^2\beta^2(D_{12} + 2D_{66})) +\\&\quad K_w + G_p(\alpha^2+\beta^2) + \left(\frac{K_lK_u}{K_l+K_u}\right) + \left(\frac{K_sK_u}{K_l+K_u}\right)(\alpha^2+\beta^2)\\&S_{34} = -(\alpha^4k_1A'D_{11}^s + \beta^4k_2B'D_{22}^s) -\\&\quad \alpha^2\beta^2(k_1A' + k_2B')(D_{12}^s + 2D_{66}^s) + L^a(\alpha^2+\beta^2)\\&S_{44} = \alpha^4\left(k_1A'\right)^2H_{11}^s + \beta^4(k_2B')^2H_{22}^s +\\&\quad (2k_1k_2A'B'H_{12}^s + (k_1A' + k_2B')^2H_{66}^s)\alpha^2\beta^2\\&\quad + \alpha^2((k_1A')^2F_{55}^s + 2k_1A'X_{55}^s + A_{55}^s) +\\&\quad \beta^2((k_2B')^2F_{44}^s + 2k_2B'X_{44}^s + A_{44}^s)\\&\quad -2R(k_1A'\alpha^2 + k_2B'\beta^2) + R^a\end{aligned} \tag{43}$$

and

$$\begin{aligned}&m_{11} = I_0,\ m_{13} = -\alpha\,I_1,\ m_{14} = J_1k_1A'\alpha,\\&m_{22} = I_0,\ m_{23} = -\beta\,I_1,\ m_{24} = k_2B'\,\beta\,J_1,\\&m_{33} = I_0 + I_2(\alpha^2+\beta^2),\\&m_{34} = -J_2\left(k_1\,A'\alpha^2 + k_2\,B'\beta^2\right) + J_1^{st},\\&m_{44} = K_2\left(\left(k_1\,A'\right)^2\alpha^2 + \left(k_2\,B'\right)^2\beta^2\right) + K_2^{st}\end{aligned} \tag{44}$$

Table 1 Non-dimensional fundamental frequency "$\hat{w}$" of isotropic square plate (a=10, ν=0.3, h/a=0.1, E=30×10^6)

Model	Var.	Mode (m, n)						
		(1, 1)	(1, 2)	(2, 2)	(2, 3)	(3, 3)	(2, 4)	(1, 5)
Zhou *et al*. (2002)	-	0.0932	0.2226	0.3421	0.5239	0.6889	0.7511	0.9268
Jha *et al*. (2013)	10	0.0932	0.2226	0.3421	0.5240	0.6892	0.7515	0.9275
Akavci and Tanrikulu (2015)	6	0.0932	0.2227	0.3424	0.5247	0.6902	0.7526	0.9290
Benahmed *et al*. (2017)	5	0.0932	0.2229	0.3425	0.5248	0.6904	0.7528	0.9294
Farzam-Rad *et al*. (2017)	5	0.0932	0.2227	0.3423	0.5243	0.6896	0.7520	0.9284
Shahsavari *et al*. (2018b)	5	0.0932	0.2226	0.3421	0.5240	0.6892	0.7514	0.9274
Present	4	0.0934	0.2234	0.3436	0.5264	0.6924	0.7548	0.9318

3. Numerical results and discussion

In this part, the dynamic behavior analysis of simply supported FG-plate reposed on elastic foundations (Winkler/Pasternak/Kerr) is investigated. Several numerical results of frequency parameters for isotropic perfect and imperfect FG plate are presented in explicit tables and graphs.

For comparison, the following non-dimensional foundation parameters and fundamental natural frequencies are employed (Benahmed *et al*. 2017, Wattanasakulpong and Ungbhakorn 2014)

Frequency parameters:

$$\hat{\omega}=\omega h\sqrt{\rho/G},\ \tilde{\omega}=\omega h\sqrt{\rho_m/E_m},\ \varpi=\omega\frac{a^2}{h}\sqrt{\rho_m/E_m}, \tag{45}$$

Foundation parameters:

$$\bar{K}_w=\frac{K_w a^4}{D_{11}},\ \bar{G}_p=\frac{G_p a^2}{D_{11}},$$
$$\bar{K}_l=\frac{K_l a^4}{D_{11}},\ \bar{K}_u=\frac{K_u a^4}{D_{11}},\ \bar{K}_s=\frac{K_s a^2}{D_{11}} \tag{46}$$

With $D_{11}=\left(E_m h^3\right)/\left(12(1-\nu_m{}^2)\right)$.

3.1 Isotropic plate

The Table 1, shows the non-dimensional fundamental frequency "$\hat{\omega}$" of simply supported isotropic square plate with (h/a=0.1 and E=30.10^6). The obtained results are

Table 2 Non-dimensional fundamental frequency "$\tilde{\omega}$" of FG-plates

h/a	Model	b/a=1			b/a=2		
		p=0	p=1	p=2	p=0	p=1	p=2
0.1	Jin *et al*. (2014)	0.1135	0.0870	0.0789	0.0719	0.0550	0.0499
	Mantari *et al*. (2014)	0.1135	0.0882	0.0806	0.0718	0.0557	0.0510
	Farzam-Rad *et al*. (2017)	0.1136	0.0882	0.0806	0.0719	0.0558	0.0510
	Shahsavari *et al*. (2018b)	0.1135	0.0882	0.0806	0.0718	0.0557	0.0510
	Present	0.1138	0.0884	0.0807	0.0720	0.0558	0.0510
0.2	Jin *et al*. (2014)	0.4169	0.3222	0.2905	0.2713	0.2088	0.1888
	Mantari *et al*. (2014)	0.4168	0.3260	0.2961	0.2712	0.2115	0.1926
	Farzam-Rad *et al*. (2017)	0.4170	0.3262	0.2961	0.2714	0.2116	0.1926
	Shahsavari *et al*. (2018b)	0.4168	0.3260	0.2961	0.2720	0.2115	0.1926
	Present	0.4185	0.3272	0.2966	0.2724	0.2124	0.1929
0.5	Jin *et al*. (2014)	1.8470	1.4687	1.3095	0.9570	0.7937	0.7149
	Mantari *et al*. (2014)	1.8505	1.4774	1.3219	1.3040	1.0346	0.9293
	Farzam-Rad *et al*. (2017)	1.8528	1.4788	1.3226	0.9570	0.7961	0.7193
	Shahsavari *et al*. (2018b)	1.8503	1.4772	1.3218	1.3039	1.0345	0.9293
	Present	1.8588	1.4836	1.3254	1.3110	1.0400	0.9318

Table 3 Non-dimensional fundamental frequencies "ϖ" of square FG-plates resting on Winkler-Pasternak foundations (p=2.3, E_c/E_m=10, h/a=0.1)

$\bar{G}_p$	Model	ε_z	Var.	$\bar{K}_w$			
				0	10	100	1000
0	Lü *et al*. (2009)	≠0	-	5.1295	5.1520	5.3498	7.0281
	Benahmed *et al*. (2017)	≠0	5	5.1638	5.1871	5.3923	7.1262
	Thai and Choi (2011)	=0	4	5.2385	5.2605	5.4548	7.1116
	Shahsavari *et al*. (2018b)	≠0	5	5.1556	5.1791	5.3855	7.1285
	Present	≠0	4	5.1637	5.1870	5.3920	7.1250
10	Lü *et al*. (2009)	≠0	-	5.5560	5.5767	5.7600	7.3450
	Benahmed *et al*. (2017)	≠0	5	5.6059	5.6274	5.8171	7.4527
	Thai and Choi (2011)	=0	4	5.6576	5.6780	5.8584	7.4257
	Shahsavari *et al*. (2018b)	≠0	5	5.6004	5.6220	5.8127	7.4565
	Present	≠0	4	5.6055	5.6269	5.8165	7.4514
25	Lü *et al*. (2009)	≠0	-	6.1404	6.1591	6.3255	7.7962
	Benahmed *et al*. (2017)	≠0	5	6.2103	6.2297	6.4015	7.9172
	Thai and Choi (2011)	=0	4	6.2336	6.2521	6.4164	7.8734
	Shahsavari *et al*. (2018b)	≠0	5	6.2080	6.2275	6.4002	7.9230
	Present	≠0	4	6.2095	6.2289	6.4006	7.9157

Table 4 Non-dimensional fundamental frequencies "$\widetilde{\omega}$" of square isotropic and FG-plates resting on Winkler-Pasternak foundations

$\overline{K}_w$	$\overline{G}_p$	h/a	Model	p = 0	0.5	1	2	5
0	0	0.05	Benahmed *et al*. (2017)	0.0291	-	0.0226	0.0207	-
			Baferani *et al*. (2011)	0.0290	0.0249	0.0227	0.0209	0.0197
			Shahsavari *et al*. (2018b)	0.0291	0.0248	0.0226	0.0206	0.0195
			Present	0.0291	0.0248	0.0226	0.0207	0.0195
		0.1	Benahmed *et al*. (2017)	0.1136	-	0.0883	0.0807	-
			Baferani *et al*. (2011)	0.1134	0.0975	0.0891	0.0819	0.0767
			Shahsavari *et al*. (2018b)	0.1135	0.0970	0.0882	0.0806	0.0755
			Present	0.1137	0.0973	0.0883	0.0806	0.0756
		0.15	Benahmed *et al*. (2017)	0.2461	-	0.1918	0.1748	-
			Baferani *et al*. (2011)	0.2454	0.2121	0.1939	0.1778	0.1648
			Shahsavari *et al*. (2018b)	0.2459	0.2109	0.1916	0.1746	0.1622
			Present	0.2466	0.2116	0.1921	0.1748	0.1624
		0.2	Benahmed *et al*. (2017)	0.4174	-	0.3264	0.2965	-
			Baferani *et al*. (2011)	0.4154	0.3606	0.3299	0.3016	0.2765
			Shahsavari *et al*. (2018b)	0.4168	0.3586	0.3260	0.2961	0.2722
			Present	0.4184	0.3602	0.3272	0.2966	0.2726
100	0	0.05	Benahmed *et al*. (2017)	0.0298	-	0.0236	0.0218	-
			Baferani *et al*. (2011)	0.0298	0.0258	0.0238	0.0221	0.0210
			Shahsavari *et al*. (2018b)	0.0298	0.0257	0.0236	0.0218	0.0208
			Present	0.0298	0.0257	0.0236	0.0218	0.0208
		0.1	Benahmed *et al*. (2017)	0.1164	-	0.0924	0.0854	-
			Baferani *et al*. (2011)	0.1162	0.1012	0.0933	0.0867	0.0821
			Shahsavari *et al*. (2018b)	0.1163	0.1006	0.0923	0.0853	0.0809
			Present	0.1165	0.1008	0.0924	0.0854	0.0809
		0.15	Benahmed *et al*. (2017)	0.2524	-	0.2011	0.1855	-
			Baferani *et al*. (2011)	0.2519	0.2204	0.2036	0.1889	0.1775
			Shahsavari *et al*. (2018b)	0.2522	0.2190	0.2010	0.1855	0.1745
			Present	0.2528	0.2196	0.2014	0.1856	0.1746
		0.2	Benahmed *et al*. (2017)	0.4286	-	0.3431	0.3158	-
			Baferani *et al*. (2011)	0.4273	0.3758	0.3476	0.3219	0.2999
			Shahsavari *et al*. (2018b)	0.4284	0.3734	0.3431	0.3159	0.2950
			Present	0.4298	0.3748	0.3438	0.3158	0.2948
100	100	0.05	Benahmed *et al*. (2017)	0.0411	-	0.0386	0.0383	-
			Baferani *et al*. (2011)	0.0411	0.0395	0.0388	0.0386	0.0388
			Shahsavari *et al*. (2018b)	0.0411	0.0393	0.0386	0.0383	0.0385
			Present	0.0411	0.0393	0.0386	0.0383	0.0385
		0.1	Benahmed *et al*. (2017)	0.1614	-	0.1521	0.1509	-
			Baferani *et al*. (2011)	0.1619	0.1563	0.1542	0.1535	0.1543
			Shahsavari *et al*. (2018b)	0.1616	0.1551	0.1525	0.1512	0.1521
			Present	0.1615	0.1550	0.1523	0.1510	0.1516
		0.15	Benahmed *et al*. (2017)	0.3537	-	0.3349	0.3323	-
			Baferani *et al*. (2011)	0.3560	0.3460	0.3422	0.3412	0.3427
			Shahsavari *et al*. (2018b)	0.3551	0.3421	0.3367	0.3342	0.3358
			Present	0.3544	0.3414	0.3358	0.3328	0.3336
		0.2	Benahmed *et al*. (2017)	0.6089	-	0.5794	0.5752	-
			Baferani *et al*. (2011)	0.6162	0.6026	0.5978	0.5970	0.5993
			Shahsavari *et al*. (2018b)	0.6137	0.5940	0.5856	0.5815	0.5843
			Present	0.6118	0.5920	0.5828	0.5776	0.5784

compared with those given by exact 3D solution developed by Zhou *et al*. (2002) and the existing quasi-3D theories in the literature such as ten variables quasi-3D theory published by Jha *et al*. (2013), six variables quasi-3D theory developed by Akavci and Tanrikulu (2015), and five variables quasi-3D theories of (Benahmed *et al*. 2017, Farzam-Rad *et al*. 2017, Shahsavari *et al*. 2018b). From the table, it can be seen that the present theory with only four unknown is in good agreement with exact 3D solution and others Quasi-3D theories.

3.2 Functionally graded plate (FGM)

The second part of the results is reserved for functionally graded plate. The properties of materials used in the FG-plate are the alumina Al_2O_3 (ceramic) with Young's modulus E_c=380 GPa and density E_c=3800 kg/m^3 and the second material is aluminum Al with Young's

Table 5 Non-dimensional fundamental frequencies "$\tilde{\varpi}$" of square isotropic and FG-plates resting on Kerr foundation ($\bar{K}_l = 100$)

$\bar{K}_u$	$\bar{K}_s$	*h/a*	Model	Isotropic plate		FG plate			
				Ceramic	Metal	*P*=0.5	*P*=1.0	*P*=2.0	*P*=5.0
100	0	0.05	Shahsavari *et al*. (2018b)	0.0294	0.0157	0.0253	0.0231	0.0212	0.0202
			Present	0.0295	0.0158	0.0253	0.0231	0.0213	0.0202
		0.1	Shahsavari *et al*. (2018b)	0.1149	0.0615	0.0988	0.0903	0.0830	0.0783
			Present	0.1151	0.0616	0.0991	0.0904	0.0831	0.0783
		0.15	Shahsavari *et al*. (2018b)	0.2491	0.1337	0.2149	0.1964	0.1801	0.1685
			Present	0.2498	0.1340	0.2156	0.1969	0.1803	0.1686
		0.2	Shahsavari *et al*. (2018b)	0.4226	0.2278	0.3661	0.3347	0.3061	0.2838
			Present	0.4242	0.2282	0.3676	0.3356	0.3064	0.2840
100	100	0.05	Shahsavari *et al*. (2018b)	0.0356	0.0285	0.0329	0.0316	0.0308	0.0305
			Present	0.0356	0.0284	0.0329	0.0316	0.0308	0.0305
		0.1	Shahsavari *et al*. (2018b)	0.1396	0.1125	0.1294	0.1245	0.1212	0.1201
			Present	0.1397	0.1123	0.1294	0.1245	0.1210	0.1198
		0.15	Shahsavari *et al*. (2018b)	0.3054	0.2487	0.2824	0.2740	0.2666	0.2637
			Present	0.3054	0.2476	0.2840	0.2736	0.2658	0.2624
		0.2	Shahsavari *et al*. (2018b)	0.5246	0.4332	0.4906	0.4739	0.4615	0.4560
			Present	0.5242	0.4306	0.4900	0.4726	0.4592	0.4522
200	100	0.05	Shahsavari *et al*. (2018b)	0.0375	0.0317	0.0351	0.0341	0.0335	0.0334
			Present	0.0375	0.0317	0.0351	0.0341	0.0334	0.0334
		0.1	Shahsavari *et al*. (2018b)	0.1473	0.1255	0.1385	0.1345	0.1320	0.1316
			Present	0.1473	0.1252	0.1385	0.1344	0.1318	0.1313
		0.15	Shahsavari *et al*. (2018)	0.3228	0.2779	0.3047	0.2964	0.2909	0.2897
			Present	0.3226	0.2766	0.3044	0.2958	0.2898	0.2882
		0.2	Shahsavari *et al*. (2018b)	0.5559	0.4850	0.5273	0.5139	0.5047	0.5024
			Present	0.5550	0.4816	0.5262	0.5120	0.5018	0.4978
200	200	0.05	Shahsavari *et al*. (2018b)	0.0440	0.0419	0.0427	0.0423	0.0422	0.0426
			Present	0.0440	0.0419	0.0427	0.0422	0.0422	0.0426
		0.1	Shahsavari *et al*. (2018b)	0.1735	0.1660	0.1687	0.1670	0.1668	0.1684
			Present	0.1733	0.1655	0.1685	0.1667	0.1664	0.1679
		0.15	Shahsavari *et al*. (2018b)	0.3819	0.3686	0.3728	0.3694	0.3689	0.3725
			Present	0.3810	0.3664	0.3718	0.3682	0.3672	0.3700
		0.2	Shahsavari *et al*. (2018b)	0.6617	0.5511	0.6484	0.6436	0.6431	0.6494
			Present	0.6590	0.5510	0.6454	0.6404	0.6386	0.6424

modulus E_m=70 GPa and density ρ_m=2702 Kg/m^3 and the poison's ratio's is v=0.3 for the both materials (ceramic and metal).

3.2.1 Perfect simply supported FG-plate

The Table 2 illustrates the variation of the non-dimensional frequency parameter "$\tilde{\varpi}$" of simply supported square "*b/a*=1" and rectangular "*b/a*=2" FG-plate as function of the geometry ratio "*h/a*" and material index "*p*". The current results computed using with present four variables quasi-3D theory are compared with those obtained by quasi-3D theories of (Mantari *et al*. 2014, Farzam-Rad *et al*. 2017, Shahsavari *et al*. 2018b) and the exact 3D solution developed by Jin *et al*. (2014). It can be observed from the Table that a good agreement is confirmed between the present results and those obtained by the other quasi-3D and exact 3D theories and this for moderately thick "*h/a*=0.1", thick "*h/a*=0.2" and very thick "*h/a*=0.5" square FG-plate. A small difference is noticed between the current results and those obtained via exact 3D solution and quasi 3D theory of Farzam-Rad *et al*. (2017) for a very thick rectangular FG-plate. It can also be remarkable that the non-dimensional frequency parameter "$\tilde{\varpi}$" is in direct correlation relation with the geometry ratio "*h/a*" and in inverse relation with material index "*p*".

3.2.2 Perfect FG-plates resting on elastic foundation (Winkler-Pasternak- Kerr)

The Table 3 presents the values of the non-dimensional fundamental frequencies $\bar{\varpi}$ of FG square plates resting on Winkler-Pasternak foundations with (p=2.3, E_c/E_m=10 and *h/a*=0.1). The computed frequencies using the current model are compared with those given by a quasi-3D theories with five unknowns proposed by Benahmed *et al*. (2017) and Shahsavari *et al*. (2018b), refined plate theory developed by Thai and Choi (2011) and the exact solution of Lü *et al*. (2009). From the obtained results it can be observed that the current model gives almost the same results as the five variables quasi-3D theories and exact 3D solution. It is obvious also that the increase in the values of spring constant "$\bar{K}_w$" and shear layer parameter "$\bar{G}_p$" leads to an increase in the non-dimensional fundamental frequencies, so we can conclude that the presence of the foundation makes the plate stiffer.

The Table 4 illustrates the variations of the non-dimensional fundamental frequencies "$\tilde{\varpi}$" of FG square plates versus the geometry ratios "*h/a*", material index "*p*"

Table 6 Variations of frequency parameters “ $\bar{\varpi}$ ” of perfect and imperfect FG-square plates versus the Winkler-Pasternak foundation stiffness (p=1)

($\bar{K}_w,\bar{G}_p$)	h/a	ξ	Even porosity	Uneven porosity	Logarithmic-uneven porosity	Mass-density porosity	Perfect
(0,0)	0.05	0.05	8.8888	9.0368	9.0368	8.6248	9.030
		0.1	8.7352	9.0456	9.0456	8.1224	
		0.15	8.5656	9.0552	9.0544	7.4713	
		0.2	8.3728	9.0656	9.0640	6.5652	
	0.1	0.05	8.6992	8.8408	8.8402	8.4432	8.836
		0.1	8.5520	8.8464	8.8458	7.9568	
		0.15	8.3898	8.8532	8.8526	7.3262	
		0.2	8.2058	8.8606	8.8594	6.4470	
	0.15	0.05	8.4131	8.5429	8.5426	8.1670	8.541
		0.1	8.2761	8.5456	8.5456	7.7040	
		0.15	8.1248	8.5494	8.5492	7.1036	
		0.2	7.9539	8.5542	8.5534	6.2656	
	0.2	0.05	8.0635	8.1795	8.1795	7.8280	8.180
		0.1	7.9385	8.1800	8.1800	7.3930	
		0.15	7.8015	8.1815	8.1810	6.8285	
		0.2	7.6450	8.1835	8.1830	6.0395	
(100,0)	0.05	0.05	9.3248	9.4560	9.4560	9.0736	9.439
		0.1	9.2032	9.4752	9.4744	8.6240	
		0.15	9.0696	9.4960	9.4936	8.0440	
		0.2	8.9192	9.5176	9.5136	7.2491	
	0.1	0.05	9.1372	9.2608	9.2602	8.8936	9.246
		0.1	9.0216	9.2770	9.2764	8.4588	
		0.15	8.8948	9.2950	9.2932	7.8990	
		0.2	8.7532	9.3142	9.3106	7.1298	
	0.15	0.05	8.8538	8.9654	8.9654	8.6202	8.954
		0.1	8.7480	8.9797	8.9788	8.2082	
		0.15	8.6328	8.9939	8.9930	7.6783	
		0.2	8.5037	9.0108	9.0072	6.9482	
	0.2	0.05	8.5095	8.6080	8.6080	8.2865	8.598
		0.1	8.4160	8.6195	8.6190	7.9025	
		0.15	8.3140	8.6320	8.6305	7.4075	
		0.2	8.1995	8.6455	8.6430	6.7240	
(100,100)	0.05	0.05	15.6210	15.5700	15.5680	15.4710	15.435
		0.1	15.8270	15.7100	15.7030	15.4960	
		0.15	16.0580	15.8570	15.8410	15.4990	
		0.2	16.3140	16.0100	15.9810	15.4610	
	0.1	0.05	15.4150	15.3570	15.3560	15.2690	15.226
		0.1	15.6250	15.4950	15.4880	15.3030	
		0.15	15.8600	15.6390	15.6230	15.3160	
		0.2	16.1210	15.7900	15.7610	15.2900	
	0.15	0.05	15.1180	15.0520	15.0500	14.9780	14.924
		0.1	15.3340	15.1860	15.1800	15.0240	
		0.15	15.5730	15.3260	15.3100	15.0520	
		0.2	15.8380	15.4730	15.4450	15.0390	
	0.2	0.05	14.7730	14.6990	14.6980	14.6420	14.574
		0.1	14.9930	14.8300	14.8230	14.7020	
		0.15	15.2360	14.9660	14.9510	14.7430	
		0.2	15.5060	15.1080	15.0820	14.7430	

and stiffness parameters of Winkler-Pasternak foundation ($\bar{K}_w,\bar{G}_p$). The current results are compared with those presented by Benahmed *et al*. (2017), Baferani *et al*. (2011) and Shahsavari *et al*. (2018b). It can be seen from the table that a good agreement is confirmed between the present results and those of the models existing in the literature. It can be also remarkable that the non-dimensional fundamental frequencies “$\tilde{\varpi}$” are in direct correlation relation with the geometry ratios “*h/a*”. It is noticed also that the power index “*p*” has a slight influence on the fundamental frequencies “$\tilde{\varpi}$”. It is confirmed from the results that the presence of the elastic foundation leads to an increase in the frequency parameter “$\tilde{\varpi}$”.

The Table 5 shows the effect of Kerr foundation on the non-dimensional fundamental frequencies “$\tilde{\varpi}$” of isotropic (all ceramic and all metallic) and FG square plates for various values of power index “*p*”, thickness ratios “*h/a*”, upper spring and shear layer parameters ($\bar{K}_u,\bar{K}_s$). The

Table 7 Variations of frequency parameters "$\bar{\omega}$" of perfect and imperfect FG-square plates versus the Kerr foundation stiffness (p=1, $\bar{K}_l=100$)

$(\bar{K}_u, \bar{K}_s)$	*h/a*	ξ	Even porosity	Uneven porosity	Logarithmic-uneven porosity	Mass-density porosity	Perfect
(100,0)	0.05	0.05	9.1096	9.2488	9.2488	8.8520	9.2368
		0.1	8.9720	9.2632	9.2624	8.3768	
		0.15	8.8208	9.2784	9.2768	7.7630	
		0.2	8.6504	9.2944	9.2912	6.9156	
	0.1	0.05	8.9210	9.0532	9.0526	8.6712	9.0434
		0.1	8.7898	9.0644	9.0638	8.2114	
		0.15	8.6464	9.0770	9.0750	7.6182	
		0.2	8.4842	9.0906	9.0874	6.7974	
	0.15	0.05	8.6365	8.7568	8.7568	8.3968	8.7496
		0.1	8.5152	8.7651	8.7648	7.9602	
		0.15	8.3827	8.7748	8.7737	7.3966	
		0.2	8.2333	8.7855	8.7833	6.6157	
	0.2	0.05	8.2895	8.3965	8.3965	8.0605	8.3915
		0.1	8.1810	8.4025	8.4020	7.6520	
		0.15	8.0620	8.4100	8.4090	7.1240	
		0.2	7.9270	8.4175	8.4160	6.3910	
(100,100)	0.05	0.05	12.7090	12.7300	12.7290	12.5250	12.645
		0.1	12.7830	12.8180	12.8140	12.3710	
		0.15	12.8690	12.9120	12.9020	12.1660	
		0.2	12.9660	13.0100	12.9910	11.8780	
	0.1	0.05	12.5160	12.5310	12.5290	12.3380	12.449
		0.1	12.5960	12.6170	12.6130	12.1960	
		0.15	12.6880	12.7080	12.6980	12.0060	
		0.2	12.7920	12.8030	12.7850	11.7340	
	0.15	0.05	12.2340	12.2380	12.2370	12.0640	12.159
		0.1	12.3210	12.3220	12.3180	11.9400	
		0.15	12.4210	12.4100	12.4000	11.7700	
		0.2	12.5330	12.5020	12.4850	11.5220	
	0.2	0.05	11.9020	11.8960	11.8940	11.7410	11.818
		0.1	11.9980	11.9760	11.9720	11.6380	
		0.15	12.1060	12.0620	12.0520	11.4920	
		0.2	12.2260	12.1510	12.1340	11.2700	
(200,100)	0.05	0.05	13.7480	13.7420	13.7410	13.5780	13.639
		0.1	13.8720	13.8500	13.8440	13.4940	
		0.15	14.0130	13.9620	13.9500	13.3700	
		0.2	14.1700	14.0820	14.0580	13.1810	
	0.1	0.05	13.5510	13.5380	13.5370	13.3870	13.438
		0.1	13.6810	13.6440	13.6380	13.3130	
		0.15	13.8260	13.7550	13.7420	13.2020	
		0.2	13.9890	13.8700	13.8480	13.0280	
	0.15	0.05	13.2650	13.2430	13.2420	13.1080	13.146
		0.1	13.4010	13.3450	13.3410	13.0490	
		0.15	13.5530	13.4530	13.4410	12.9570	
		0.2	13.7240	13.5660	13.5440	12.8030	
	0.2	0.05	12.9300	12.8980	12.8970	12.7820	12.804
		0.1	13.0720	12.9980	12.9920	12.7410	
		0.15	13.2320	13.1020	13.0900	12.6690	
		0.2	13.4090	13.2110	13.1900	12.5360	

results computed using the current four variable quasi-3D theory are almost identical to those given via quasi-3D theory (with five unknown) of Shahsavari *et al.* (2018b).

It can be seen from the table that the non-dimensional fundamental frequencies "$\tilde{\omega}$" increase with increasing of upper spring and shear layer parameters $(\bar{K}_u, \bar{K}_s)$. It can also be noted that the presence of the upper spring "$\bar{K}_u$" in the foundation of Kerr makes the plate stiffer, we can also confirm that the power-law index "p" has a slight influence on the results. The biggest values of the non-dimensional frequency are obtained for fully ceramic plate and this is due to the high rigidity of ceramic.

3.2.3 Perfect and imperfect FG-plates resting on Winkler-Pasternak-Kerr elastic foundation

In this section, the presence of the porosity in the material that makes up the FG-plate is considered. Four model of distribution of the micro-voids is examined and presented in the following.

Table 7 Continued

$(\bar{K}_u, \bar{K}_s)$	*h/a*	ξ	Even porosity	Uneven porosity	Logarithmic-uneven porosity	Mass-density porosity	Perfect
(200,200)	0.05	0.05	17.138	17.0540	17.0520	17.0020	16.895
		0.1	17.406	17.2190	17.2100	17.1050	
		0.15	17.703	17.3910	17.3730	17.1980	
		0.2	18.033	17.5720	17.5380	17.2640	
	0.1	0.05	16.922	16.8320	16.8300	16.7890	16.677
		0.1	17.195	16.9950	16.9870	16.9000	
		0.15	17.495	17.1650	17.1460	17.0010	
		0.2	17.828	17.3420	17.3080	17.0770	
	0.15	0.05	16.614	16.5170	16.5140	16.4860	16.365
		0.1	16.889	16.6750	16.6670	16.6070	
		0.15	17.193	16.8400	16.8220	16.7190	
		0.2	17.53	17.0140	16.9800	16.8050	
	0.2	0.05	16.259	16.1540	16.1520	16.1380	16.006
		0.1	16.537	16.3080	16.3010	16.2700	
		0.15	16.843	16.4700	16.4520	16.3920	
		0.2	17.18	16.6380	16.6060	16.4820	

The Table 6 presents the effects of the imperfection (porosity) and the Winkler-Pasternak foundation on the frequency parameters " $\bar{\omega}$ " of the thin, moderately thick and thick square FG-plates with " $p=1$ ". It can be observed from the tabulated results that the increase in volume fraction porosity of the uneven and logarithmic-uneven porosities model has a slight effect on the values of frequency parameters " $\bar{\omega}$ " but the mass-density porosities model has a significant influence when the parameter of porosity " ξ " increases.

It can also be noted from the table that the frequency parameter $\bar{\omega}$ is in relation inverse with the porosity volume fraction "ξ" of even and mass-density porosities models but in the case of uneven and logarithmic-uneven porosities the frequency parameter $\bar{\omega}$ increase with increasing of "ξ" even it exceeds the frequency parameter of the perfect plate. It is concluded again that the higher values of the frequency $\bar{\omega}$ is obtained for the plates resting on elastic foundation with $(\bar{K}_w, \bar{G}_p = 100)$.

The variations of the frequency parameters $\bar{\omega}$ of perfect and imperfect FG square plates as function of the Kerr foundation stiffness is presented in the Table 7. The power law index is considered equal one "*p*=1", and the lower spring stiffness " $\bar{K}_l = 100$ ".

The current results are computed with various distributions of the porosities through the thickness of the plate (even, uneven, logarithmic uneven and mass density porosities). It can be noted from the obtained results that the increase in the Kerr foundation stiffness ($\bar{K}_u, \bar{K}_s$) leads to an increase in the frequency $\bar{\omega}$. For the even and masse density models, it is confirmed that the frequency parameter $\bar{\omega}$ decreases with increasing of the porosity volume fraction "ξ" but for uneven and logarithmic models this is reversed.

Fig. 3 illustrates the variation of the non-dimensional frequency " $\bar{\omega}$ " of the perfect and imperfect FG-plates resting on the elastic foundation versus the thickness ratio "*a/h*" and the spring constant " $\bar{K}_w$ " with $(\bar{G}_p = 10 \; and \; \xi = 0.05)$. It can be seen from the plotted

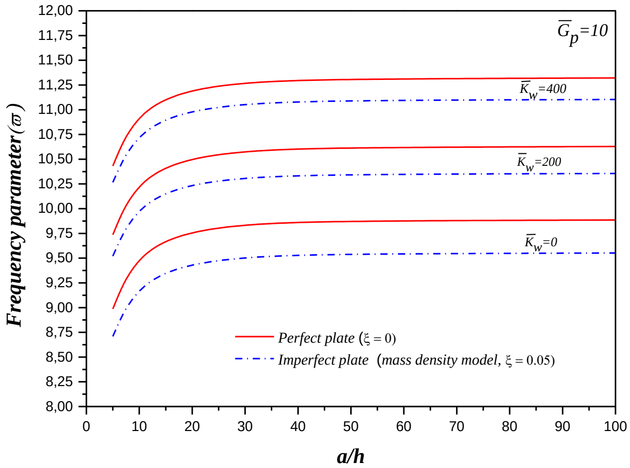

Fig. 3 The variation of the non-dimensional frequency " $\bar{\omega}$ " of the perfect and imperfect FG-plates versus the thickness ratio "*a/h*" and the spring constant " $\bar{K}_w$ " with $(\bar{G}_p = 10 \, , p = 1 \; and \; \xi = 0.05)$

graphs that the non-dimensional frequency " $\bar{\omega}$ " increase with increasing of the geometry ratio "*a/h*" and values of the Winkler constant " $\bar{K}_w$ ".

It is clear in the graphs that the existence of the porosity (mass density model) leads to a decrease in the values of the non-dimensional frequency " $\bar{\omega}$ ".

The effect of the shear layer parameters " $\bar{G}_p$ " and the geometry ratio "*a/h*" on the non-dimensional frequency " $\bar{\omega}$ " of perfect and imperfect FG-plates is plotted in the Fig. 4. The value of the spring constant is considered " $\bar{K}_w = 100$ ". The plotted curves of imperfect FG-plate are computed via mass density model with "ξ=0.05". From the graphs it can be noted that the increase of the shear layer parameters " $\bar{G}_p$ " leads to an increase in the values of non-dimensional frequency " $\bar{\omega}$ ". For the great values of " $\bar{G}_p$ ", it is remarkable that the frequency results of the perfect and imperfect plate converge.

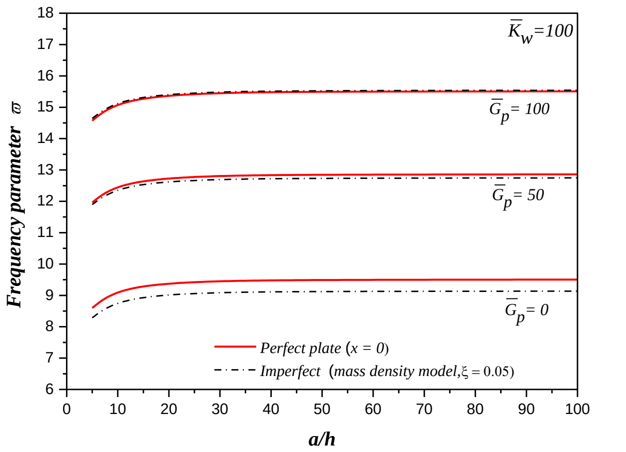

Fig. 4 The effect of the shear layer parameters "$\bar{G}_p$" and the geometry ratio "*a/h*" on the non-dimensional frequency "ϖ" of perfect and imperfect FG-plates with ($\bar{K}_w = 100$ *and* $p = 1$)

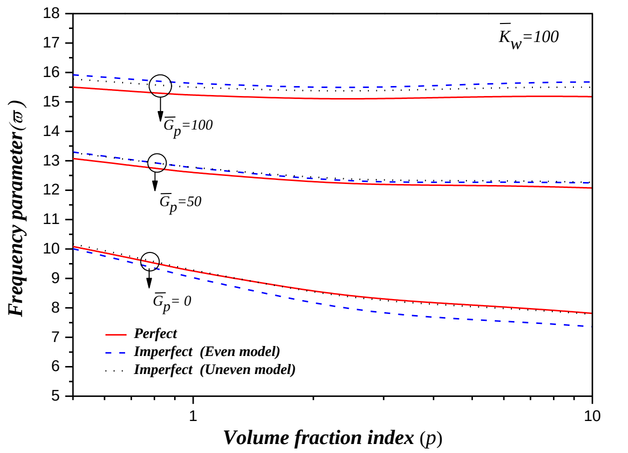

Fig. 6 The effect of the power index "*p*" and shear layer parameters "$\bar{G}_p$" on the non-dimensional frequency "ϖ" of perfect and imperfect FG-plates with ($\bar{K}_w = 100$, *a/h*=10 and ξ=0.1)

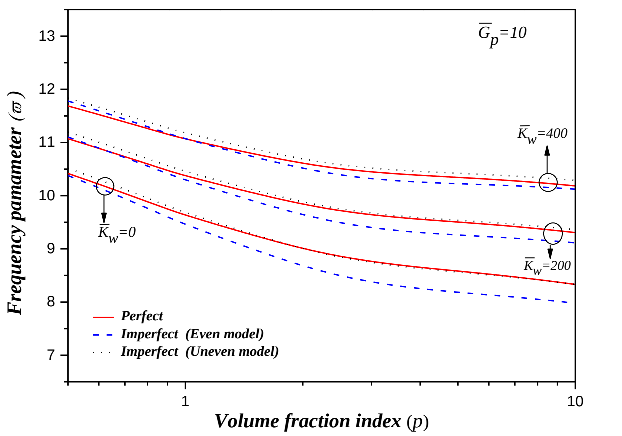

Fig. 5 The variation of the non-dimensional frequency "ϖ" of perfect and imperfect plate versus the power index *p* and the spring constant "$\bar{K}_w$" with ($\bar{G}_p = 10$, *a/h*=10 and ξ=0.1)

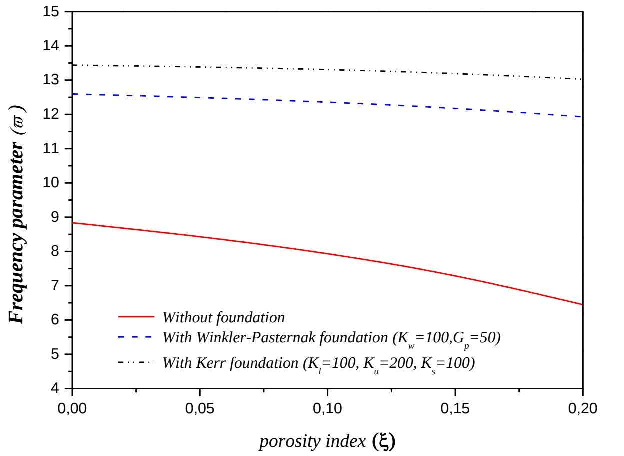

Fig. 7 The effect of the elastic foundation and the porosity index "ξ" on the frequency parameter "ϖ" with (*a/h*=10 and *p*=1)

The variation of the non-dimensional frequency "ϖ" of perfect and imperfect plate versus the power index p and the spring constant "$\bar{K}_w$" is presented in Fig. 5. The shear layer parameters is taken "$\bar{G}_p = 10$" and porosity volume fraction "ξ=0.1". It can be seen from the obtained curves that the values of the non-dimensional frequency "ϖ" decrease with the increase of the power index "*p*". The greater values of the frequency parameter are obtained for the FG-plate resting on elastic foundation with ($\bar{K}_w = 400, \bar{G}_p = 10$).

Fig. 6 shows the effect of the power index "*p*" and shear layer parameters "$\bar{G}_p$" on the non-dimensional frequency "ϖ" of perfect and imperfect FG-plates with ($\bar{K}_w = 100$ and ξ=0.1). From the plotted graphs it can be concluded that the non-dimensional frequency "ϖ" is in direct correlation relation with the shear layer parameters "$\bar{G}_p$" and in inverse relation with power index "*p*".

Fig. 7 illustrates the effect of the elastic foundation and the porosity index "ξ" on the frequency parameter "ϖ". From the figure it can be seen that the elastic foundation has a significant effect on the frequency"ϖ". It is clear also that the presence of the upper spring in the elastic foundation (Kerr foundation) gives the greater values of frequency "ϖ" and this is due that the rigidity of the FG-plate increase. We can also conclude that the frequency "ϖ" decrease with increasing of the porosity volume fraction "ξ".

4. Conclusions

In this paper, a hyperbolic four variables quasi-3D theory has been presented for dynamic behavior analysis of perfect and imperfect FG-plate resting on Winkler-Pasternak-Kerr elastic foundation. Four different models of porosity distributions are considered for describing porosity effect in graded material characteristics. The equations of motion of the present problem are derived using the Hamilton's energy principle and solved via Navier solutions. The accuracy and efficiency of the present model are ascertained by comparing it with other theories, and excellent agreement was observed in all examples. We can finally conclude that the presence of the micro voids in the material has a significant effect on the frequency parameter of simply supported FG-plate. An improvement of the present formulation will be considered in the future work to consider other type of materials (Daouadji 2017, Klouche *et al*. 2017, Yeghnem *et al*. 2017, Karami *et al*. 2017, Khetir *et al*. 2017, Panjehpour *et al*. 2018, Behera and Kumari 2018, Shahadat *et al*. 2018, Karami *et al*. 2018d, Ayat *et al*. 2018, Kaci *et al*. 2018, Kadari *et al*. 2018, Cherif *et al*. 2018, Bouadi *et al*. 2018, Karami *et al*. 2018e, f, Yazid *et al*. 2018, Zine *et al*. 2018, Bensaid *et al*. 2018, Mokhtar *et al*. 2018, Hussain and Naeem 2019, Draiche *et al*. 2019, Rajabi and Mohammadimehr 2019, Fadoun2019, Benmansour *et al*. 2019, Bensattalah *et al*. 2019, Berghouti *et al*. 2019, Medani *et al*. 2019, Boutaleb *et al*. 2019, Karami *et al*. 2019c, Hussain *et al*. 2019).

References

Abdelaziz, H.H., Ait Amar Meziane, M., Bousahla, A.A., Tounsi, A., Mahmoud, S.R. and Alwabli, A.S. (2017), "An efficient hyperbolic shear deformation theory for bending, buckling and free vibration of FGM sandwich plates with various boundary conditions", *Steel Compos. Struct*., **25**(6), 693-704. https://doi.org/10.12989/scs.2017.25.6.693.

Abualnour, M., Houari, M.S.A., Tounsi, A., Bedia, E.A.A. and Mahmoud, S.R. (2018), "A novel quasi-3D trigonometric plate theory for free vibration analysis of advanced composite plates", *Compos. Struct.*, **184**, 688-697. https://doi.org/10.1016/j.compstruct.2017.10.047.

Ait Atmane, H., Tounsi, A., Bernard, F. and Mahmoud, S. (2015), "A computational shear displacement model for vibrational analysis of functionally graded beams with porosities", *Steel Compos. Struct*., **19**, 369-384. https://doi.org/10.12989/scs.2015.19.2.369.

Ait Sidhoum, I., Boutchicha, D., Benyoucef, S. and Tounsi, A. (2018), "A novel quasi-3D hyperbolic shear deformation theory for vibration analysis of simply supported functionally graded plates", *Smart Struct. Syst*., **22**(3), 303-314. https://doi.org/10.12989/sss.2018.22.3.303.

Ait Sidhoum, I., Boutchicha, D., Benyoucef, S. and Tounsi, A. (2017), "An original HSDT for free vibration analysis of functionally graded plates", *Steel Compos. Struct*., **25**(6), 735-745. https://doi.org/10.12989/scs.2017.25.6.735.

Akavci, S. and Tanrikulu, A. (2015), "Static and free vibration analysis of functionally graded plates based on a new quasi-3D and 2D shear deformation theories", *Compos. Part B, Eng*., **83**, 203-215. https://doi.org/10.1016/j.compositesb.2015.08.043.

Akbaş, Ş.D. (2017), "Vibration and static analysis of functionally graded porous plates", *J. Appl. Comput. Mech.*, **3**(3), 199-207. https://doi.org/10.22055/JACM.2017.21540.1107.

Akbaş, Ş.D. (2018), "Forced vibration analysis of functionally graded porous deep beams", *Compos. Struct.*, **186**, 293-302. https://doi.org/10.1016/j.compstruct.2017.12.013.

Akhavan, H., Hashemi, S.H., Taher, H.R.D., Alibeigloo, A. and Vahabi, S. (2009), "Exact solutions for rectangular Mindlin plates under in-plane loads resting on Pasternak elastic foundation. Part II: Frequency analysis", *Comput. Mater. Sci*., **44**, 951-961. https://doi.org/10.1016/j.commatsci.2008.07.001.

Al-Basyouni, K.S., Tounsi, A. and Mahmoud, S.R. (2015), "Size dependent bending and vibration analysis of functionally graded micro beams based on modified couple stress theory and neutral surface position", *Compos. Struct*., **125**, 621-630. https://doi.org/10.1016/j.compstruct.2014.12.070.

Aqida, S., Ghazali, M. and Hashim, J. (2004), "Effects of porosity on mechanical properties of metal matrix composite: an overview", *J. Teknol*, **40**(1), 17-32. https://doi.org/10.11113/jt.v40.395.

Arshid, E., Khorshidvand, A.R. and Khorsandijou, S.M. (2019), "The effect of porosity on free vibration of SPFG circular plates resting on visco-Pasternak elastic foundation based on CPT, FSDT and TSDT", *Struct. Eng. Mech.*, **70**(1), 97-112. https://doi.org/10.12989/sem.2019.70.1.097.

Attia, A., Bousahla, A.A., Tounsi, A., Mahmoud, S.R. and Alwabli, A.S. (2018), "A refined four variable plate theory for thermoelastic analysis of FGM plates resting on variable elastic foundations", *Struct. Eng. Mech*., **65**(4), 453-464. https://doi.org/10.12989/sem.2018.65.4.453.

Attia, A., Tounsi, A., Adda Bedia, E.A. and Mahmoud, S. (2015), "Free vibration analysis of functionally graded plates with temperature-dependent properties using various four variable refined plate theories", *Steel Compos. Struct*., **18**, 187-212. https://doi.org/10.12989/scs.2015.18.1.187.

Avcar, M. (2016), "Effects of material non-homogeneity and two parameter elastic foundation on fundamental frequency parameters of Timoshenko beams", *Acta Physica Polonica A*, **130**(1), 375-378. https://doi.org/10.12693/APhysPolA.130.375.

Avcar, M. (2019), "Free vibration of imperfect sigmoid and power law functionally graded beams", *Steel Compos. Struct.*, **30**(6), 603-615. https://doi.org/10.12989/scs.2019.30.6.603.

Avcar, M. and Mohammed, W.K.M. (2018), "Free vibration of functionally graded beams resting on Winkler-Pasternak foundation", *Arab. J. Geosci.*, **11**(10), 232. https://doi.org/10.1007/s12517-018-3579-2.

Ayat, H., Kellouche, Y., Ghrici, M. and Boukhatem, B. (2018), "Compressive strength prediction of limestone filler concrete using artificial neural networks", *Adv. Comput. Des.*, **3**(3), 289-302. https://doi.org/10.12989/acd.2018.3.3.289.

Baferani, A.H., Saidi, A. and Ehteshami, H. (2011), "Accurate solution for free vibration analysis of functionally graded thick rectangular plates resting on elastic foundation", *Compos. Struct*., **93**(7), 1842-1853. https://doi.org/10.1016/j.compstruct.2011.01.020.

Bakhadda, B., Bachir Bouiadjra, M., Bourada, F., Bousahla, A.A., Tounsi, A. and Mahmoud, S.R. (2018), "Dynamic and bending analysis of carbon nanotube-reinforced composite plates with elastic foundation", *Wind Struct.*, **27**(5), 311-324. https://doi.org/10.12989/was.2018.27.5.311.

Batou, B., Nebab, M., Bennai, R., Ait Atmane, H., Tounsi, A., Bouremana, M. and Tounsi, A. (2019), "Wave dispersion properties in imperfect sigmoid plates using various HSDTs", *Steel Compos. Struct*. (Accepted)

Behera, S. and Kumari, P. (2018), "Free vibration of Levy-type rectangular laminated plates using efficient zig-zag theory", *Adv. Comput. Des.*, **3**(3), 213-232. https://doi.org/10.12989/acd.2018.3.3.213.

Belabed, Z., Bousahla, A.A., Houari, M.S.A., Tounsi, A. and Mahmoud, S.R. (2018), "A new 3-unknown hyperbolic shear deformation theory for vibration of functionally graded sandwich plate", *Earthq. Struct.*, **14**(2), 103-115. https://doi.org/10.12989/eas.2018.14.2.103.

Belabed, Z., Houari, M.S.A., Tounsi, A., Mahmoud, S.R. and Anwar Bég, O. (2014), "An efficient and simple higher order shear and normal deformation theory for functionally graded material (FGM) plates", *Compos. Part B*, **60**, 274-283. https://doi.org/10.1016/j.compositesb.2013.12.057.

Beldjelili, Y., Tounsi, A. and Mahmoud, S.A. (2016), "Hygro-thermo-mechanical bending of S-FGM plates resting on variable elastic foundations using a four-variable trigonometric plate theory", *Smart Struct. Syst*., **18**, 755-786. https://doi.org/10.12989/sss.2016.18.4.755.

Belkorissat, I., Houari, M.S.A., Tounsi, A., Adda Bedia, E.A. and Mahmoud, S.R. (2015), "On vibration properties of functionally graded nano-plate using a new nonlocal refined four variable model", *Steel Compos. Struct*., **18**(4), 1063-1081. https://doi.org/10.12989/scs.2015.18.4.1063.

Bellifa, H., Bakora, A., Tounsi, A., Bousahla, A.A. and Mahmoud, S.R. (2017a), "An efficient and simple four variable refined plate theory for buckling analysis of functionally graded plates", *Steel Compos. Struct*., **25**(3), 257-270. https://doi.org/10.12989/scs.2017.25.3.257.

Bellifa, H., Benrahou, K.H., Bousahla, A.A., Tounsi, A. and Mahmoud, S.R. (2017b), "A nonlocal zeroth-order shear deformation theory for nonlinear postbuckling of nanobeams", *Struct. Eng. Mech*., **62**(6), 695-702. https://doi.org/10.12989/sem.2017.62.6.695.

Bellifa, H., Benrahou, K.H., Hadji, L., Houari, M.S.A. and Tounsi, A. (2016), "Bending and free vibration analysis of functionally graded plates using a simple shear deformation theory and the concept the neutral surface position", *J. Brazil. Soc. Mech. Sci. Eng*., **38**(1), 265-275. https://doi.org/10.1007/s40430-015-0354-0.

Benadouda, M., Ait Atmane, H., Tounsi, A., Bernard, F. and Mahmoud, S.R. (2017), "An efficient shear deformation theory for wave propagation in functionally graded material beams with porosities", *Earthq. Struct*., **13**(3), 255-265. https://doi.org/10.12989/eas.2017.13.3.255.

Benahmed, A., Houari, M.S.A., Benyoucef, S., Belakhdar, K and Tounsi, A. (2017), "A novel quasi-3D hyperbolic shear deformation theory for functionally graded thick rectangular plates on elastic foundation", *Geomech. Eng*., **12**(1), 9-34. https://doi.org/10.12989/gae.2017.12.1.009.

Benchohra, M., Driz, H., Bakora, A., Tounsi, A., Adda Bedia, E.A. and Mahmoud, S.R. (2018), "A new quasi-3D sinusoidal shear deformation theory for functionally graded plates", *Struct. Eng. Mech*., **65**(1), 19-31. https://doi.org/10.12989/sem.2018.65.1.019.

Bendaho, B., Belabed, Z., Bourada, M., Benatta, M.A., Bourada, F. and Tounsi, A. (2019), "Assessment of new 2D and quasi-3D nonlocal theories for free vibration analysis of size-dependent functionally graded (FG) nanoplates", *Adv. Nano Res*., **7**(4), 279-294. https://doi.org/10.12989/anr.2019.7.4.277.

Benferhat, R., Daouadji, T.H., Mansour, M.S. and Hadji, L. (2016b), "Effect of porosity on the bending and free vibration response of functionally graded plates resting on Winkler-Pasternak foundations", *Earthq. Struct*., **10**(6), 1429-1449. https://doi.org/10.12989/eas.2016.10.6.1429.

Benferhat, R., Hassaine Daouadji, T., Hadji, L. and Said Mansour, M. (2016a), "Static analysis of the FGM plate with porosities", *Steel Compos. Struct*., **21**(1), 123-136. https://doi.org/10.12989/scs.2016.21.1.123.

Benmansour, D.L., Kaci, A., Bousahla, A.A., Heireche, H., Tounsi, A., Alwabli, A.S., Alhebshi, A.M., Al-Ghmady, K. and Mahmoud, S.R. (2019), "The nano scale bending and dynamic properties of isolated protein microtubules based on modified strain gradient theory", *Adv. Nano Res.* (Accepted)

Bennai, R., Atmane, H.A. and Tounsi, A. (2015), "A new higher-order shear and normal deformation theory for functionally graded sandwich beams", *Steel Compos. Struct.*, **19**(3), 521-546. https://doi.org/10.12989/scs.2015.19.3.521.

Bennoun, M., Houari, M.S.A. and Tounsi, A. (2016), "A novel five variable refined plate theory for vibration analysis of functionally graded sandwich plates", *Mech. Adv. Mater. Struct*., **23**(4), 423-431. https://doi.org/10.1080/15376494.2014.984088.

Bensaid, I., Bekhadda, A. and Kerboua, B. (2018), "Dynamic analysis of higher order shear-deformable nanobeams resting on elastic foundation based on nonlocal strain gradient theory", *Adv. Nano Res*., **6**(3), 279-298. https://doi.org/10.12989/anr.2018.6.3.279.

Bensattalah, T., Zidour, M. and Daouadji, T.S. (2019), "A new nonlocal beam model for free vibration analysis of chiral single-walled carbon nanotubes", *Compos. Mater. Eng*., **1**(1), 21-31.

Berghouti, H., AddaBedia, E.A. Benkhedda, A. and Tounsi, A. (2019), "Vibration analysis of nonlocal porous nanobeams made of functionally graded material", *Adv. Nano Res.* (Accepted)

Bessaim, A., Houari, M.S.A., Tounsi, A., Mahmoud, S.R. and AddaBedia, E.A. (2013), "A new higher order shear and normal deformation theory for the static and free vibration analysis of sandwich plates with functionally graded isotropic face sheets", *J. Sandw. Struct. Mater*., **15**, 671-703. https://doi.org/10.1177/1099636213498888.

Besseghier, A., Houari, M.S.A., Tounsi, A. and Mahmoud, S.R. (2017), "Free vibration analysis of embedded nanosize FG plates using a new nonlocal trigonometric shear deformation theory", *Smart Struct. Syst*., **19**(6), 601-614. https://doi.org/10.12989/sss.2017.19.6.601.

Bouadi, A., Bousahla, A.A., Houari, M.S.A., Heireche, H. and Tounsi, A. (2018), "A new nonlocal HSDT for analysis of stability of single layer graphene sheet", *Adv. Nano Res*., **6**(2), 147-162. https://doi.org/10.12989/anr.2018.6.2.147.

Bouafia, K., Kaci, A., Houari, M.S.A., Benzair, A. and Tounsi, A. (2017), "A nonlocal quasi-3D theory for bending and free flexural vibration behaviors of functionally graded nanobeams", *Smart Struct. Syst*., **19**(2), 115-126. https://doi.org/10.12989/sss.2017.19.2.115.

Bouanati, S., Benrahou, K.H., Ait Atmane, H., AitYahia, S., Bernard, F., Tounsi, A. and Adda Bedia, E.A. (2019), "Investigation of wave propagation in anisotropic plates via quasi 3D HSDT", *Geomech. Eng*., **18**(1), 85-96. https://doi.org/10.12989/gae.2019.18.1.085.

Bouderba, B., Houari, M.S.A. and Tounsi, A. (2013), "Thermomechanical bending response of FGM thick plates resting on Winkler-Pasternak elastic foundations", *Steel Compos. Struct*., **14**(1), 85-104. https://doi.org/10.12989/scs.2013.14.1.085.

Bouderba, B., Houari, M.S.A., Tounsi, A. and Mahmoud, S.R. (2016), "Thermal stability of functionally graded sandwich plates using a simple shear deformation theory", *Struct. Eng. Mech*., **58**(3), 397-422. https://doi.org/10.12989/sem.2016.58.3.397.

Bouhadra, A., Tounsi, A., Bousahla, A.A., Benyoucef, S. and Mahmoud, S.R. (2018), "Improved HSDT accounting for effect of thickness stretching in advanced composite plates", *Struct. Eng. Mech*., **66**(1), 61-73. https://doi.org/10.12989/sem.2018.66.1.061.

Boukhari, A., AitAtmane, H., Houari, M.S.A., Tounsi, A., AddaBedia, E.A. and Mahmoud, S.R. (2016), "An efficient shear deformation theory for wave propagation of functionally graded material plates", *Struct. Eng. Mech*., **57**(5), 837-859. https://doi.org/10.12989/sem.2016.57.5.837.

Boukhlif, Z., Bouremana, M., Bourada, F., Bousahla, A.A., Bourada, M., Tounsi, A. and Al-Osta, M.A. (2019), "A simple quasi-3D HSDT for the dynamics analysis of FG thick plate on elastic foundation", *Steel Compos. Struct*., **31**(5), 503-516. https://doi.org/10.12989/scs.2019.31.5.503.

Boulefrakh, L., Hebali, H., Chikh, A., Bousahla, A.A., Tounsi, A. and Mahmoud, S.R. (2019), "The effect of parameters of visco-

Pasternak foundation on the bending and vibration properties of a thick FG plate", *Geomech. Eng.*, **18**(2), 161-178. https://doi.org/10.12989/gae.2019.18.2.161.

Bounouara, F., Benrahou, K.H., Belkorissat, I. and Tounsi, A. (2016), "A nonlocal zeroth-order shear deformation theory for free vibration of functionally graded nanoscale plates resting on elastic foundation", *Steel Compos. Struct.*, **20**(2), 227-249. https://doi.org/10.12989/scs.2016.20.2.227.

Bourada, F., Amara, K. and Tounsi, A. (2016), "Buckling analysis of isotropic and orthotropic plates using a novel four variable refined plate theory", *Steel Compos. Struct.*, **21**(6), 1287-1306. https://doi.org/10.12989/scs.2016.21.6.1287.

Bourada, F., Amara, K., Bousahla, A.A., Tounsi, A. and Mahmoud, S.R. (2018), "A novel refined plate theory for stability analysis of hybrid and symmetric S-FGM plates", *Struct. Eng. Mech.*, **68**(6), 661-675. https://doi.org/10.12989/sem.2018.68.6.661.

Bourada, F., Bousahla, A.A., Bourada, M., Azzaz, A., Zinata, A. and Tounsi, A. (2019), "Dynamic investigation of porous functionally graded beam using a sinusoidal shear deformation theory", *Wind Struct.*, **28**(1), 19-30. https://doi.org/10.12989/was.2019.28.1.019.

Bourada, M., Kaci, A., Houari, M.S.A. and Tounsi, A. (2015), "A new simple shear and normal deformations theory for functionally graded beams", *Steel Compos. Struct.*, **18**(2), 409-423. https://doi.org/10.12989/scs.2015.18.2.409.

Bousahla, A.A., Benyoucef, S., Tounsi, A. and Mahmoud, S.R. (2016), "On thermal stability of plates with functionally graded coefficient of thermal expansion", *Struct. Eng. Mech.*, **60**(2), 313-335. https://doi.org/10.12989/sem.2016.60.2.313.

Bousahla, A.A., Houari, M.S.A., Tounsi, A. and Adda Bedia, E.A. (2014), "A novel higher order shear and normal deformation theory based on neutral surface position for bending analysis of advanced composite plates", *Int. J. Comput. Meth.*, **11**(6), 1350082. https://doi.org/10.1142/S0219876213500825.

Boussoula, A., Boucham, B., Bourada, M., Bourada, F., Tounsi, A., Bousahla, A.A. and Tounsi, A. (2019), "A simple nth-order shear deformation theory for thermomechanical bending analysis of different configurations of FG sandwich plates", *Smart Struct. Syst.* (Accepted)

Boutaleb, S., Benrahou, K.H., Bakora, A., Algarni, A., Bousahla, A.A., Tounsi, A., Mahmoud, S.R. and Tounsi, A. (2019), "Dynamic Analysis of nanosize FG rectangular plates based on simple nonlocal quasi 3D HSDT", *Adv. Nano Res.*, **7**(3), 189-206. https://doi.org/10.12989/anr.2019.7.3.189.

Carrera, E., Brischetto, S., Cinefra, M. and Soave, M. (2011), "Effects of thickness stretching in functionally graded plates and shells", *Compos. Part B*, **42**, 123-133. https://doi.org/10.1016/j.compositesb.2010.10.005.

Chaabane, L.A., Bourada, F., Sekkal, M., Zerouati, S., Zaoui, F.Z., Tounsi, A., Derras, A., Bousahla, A.A. and Tounsi, A. (2019), "Analytical study of bending and free vibration responses of functionally graded beams resting on elastic foundation", *Struct. Eng. Mech.*, **71**(2), 185-196. https://doi.org/10.12989/sem.2019.71.2.185.

Cherif, R.H., Meradjah, M., Zidour, M., Tounsi, A., Belmahi, H. and Bensattalah, T. (2018), "Vibration analysis of nano beam using differential transform method including thermal effect", *J. Nano Res.*, **54**, 1-14.

Chikh, A., Tounsi, A., Hebali, H. and Mahmoud, S.R. (2017), "Thermal buckling analysis of cross-ply laminated plates using a simplified HSDT", *Smart Struct. Syst.*, **19**(3), 289-297. https://doi.org/10.12989/sss.2017.19.3.289.

Daouadji, T.H. (2017), "Analytical and numerical modeling of interfacial stresses in beams bonded with a thin plate", *Adv. Comput. Des.*, **2**(1), 57-69. https://doi.org/10.12989/acd.2017.2.1.057.

Draiche, K., Bousahla, A.A., Tounsi, A., Alwabli, A.S., Tounsi, A. and Mahmoud, S.R. (2019), "Static analysis of laminated reinforced composite plates using a simple first-order shear deformation theory", *Comput. Concrete*. (Accepted)

Draiche, K., Tounsi, A. and Mahmoud, S.R. (2016), "A refined theory with stretching effect for the flexure analysis of laminated composite plates", *Geomech. Eng.*, **11**(5), 671-690. https://doi.org/10.12989/gae.2016.11.5.671.

Draoui, A., Zidour, M., Tounsi, A. and Adim, B. (2019), "Static and dynamic behavior of nanotubes-reinforced sandwich plates using (FSDT)", *J. Nano Res.*, **57**, 117-135. https://doi.org/10.4028/www.scientific.net/JNanoR.57.117.

Ebrahimi, F., Mahmoodi, F. and Barati, M.R. (2017), "Thermo-mechanical vibration analysis of functionally graded micro/nanoscale beams with porosities based on modified couple stress theory", *Adv. Mater. Res.*, **6**(3), 279-301. https://doi.org/10.12989/amr.2017.6.3.279.

El-Haina, F., Bakora, A., Bousahla, A.A., Tounsi, A. and Mahmoud, S. (2017), "A simple analytical approach for thermal buckling of thick functionally graded sandwich plates", *Struct. Eng. Mech.*, **63**(5), 585-595. https://doi.org/10.12989/sem.2017.63.5.585.

Elmossouess, B., Kebdani, S., Bachir Bouiadjra, M. and Tounsi, A. (2017), "A novel and simple HSDT for thermal buckling response of functionally graded sandwich plates", *Struct. Eng. Mech.*, **62**(4), 401-415. https://doi.org/10.12989/sem.2017.62.4.401.

Eltaher, M.A., Fouda, N., El-Midany, T. and Sadoun, A.M. (2018), "Modified porosity model in analysis of functionally graded porous nanobeams", *J. Brazil. Soc. Mech. Sci. Eng.*, **40**, 141. https://doi.org/10.1007/s40430-018-1065-0.

Fadoun, O.O. (2019), "Analysis of axisymmetric fractional vibration of an isotropic thin disc in finite deformation", *Comput. Concrete*, **23**(5), 303-309. https://doi.org/10.12989/cac.2019.23.5.303.

Fahsi, A., Tounsi, A., Hebali, H., Chikh, A., Adda Bedia, E.A. and Mahmoud, S.R. (2017), "A four variable refined nth-order shear deformation theory for mechanical and thermal buckling analysis of functionally graded plates", *Geomech. Eng.*, **13**(3), 385-410. https://doi.org/10.12989/gae.2017.13.3.385.

Faleh, N.M., Ahmed, R.A. and Fenjan, R.M. (2018), "On vibrations of porous FG nanoshells", *Int. J. Eng. Sci.*, **133**, 1-14. https://doi.org/10.1016/j.ijengsci.2018.08.007.

Farzam-Rad, S.A., Hassani, B. and Karamodin, A. (2017), "Isogeometric analysis of functionally graded plates using a new quasi-3D shear deformation theory based on physical neutral surface", *Compos. Part B, Eng.*, **108**, 174-189. https://doi.org/10.1016/j.compositesb.2016.09.029.

Fourn, H., Ait Atmane, H., Bourada, M., Bousahla, A.A., Tounsi, A. and Mahmoud, S.R. (2018), "A novel four variable refined plate theory for wave propagation in functionally graded material plates", *Steel Compos. Struct.*, **27**(1), 109-122. https://doi.org/10.12989/scs.2018.27.1.109.

Gupta, A. and Talha, M. (2017), "Influence of porosity on the flexural and free vibration responses of functionally graded plates in thermal environment", *Int. J. Struct. Stab. Dyn.*, **18**(1), 1850013. https://doi.org/10.1142/S021945541850013X.

Gupta, A. and Talha, M. (2018), "Influence of porosity on the flexural and vibration response of gradient plate using nonpolynomial higher-order shear and normal deformation theory", *Int. J. Mech. Mater. Des.*, **14**(2), 277-296. https://doi.org/10.1007/s10999-017-9369-2.

Hachemi, H., Kaci, A., Houari, M.S.A., Bourada, M., Tounsi, A. and Mahmoud, S. (2017), "A new simple three-unknown shear deformation theory for bending analysis of FG plates resting on elastic foundations", *Steel Compos. Struct.*, **25**(6), 717-726. https://doi.org/10.12989/scs.2017.25.6.717.

Hamidi, A., Houari, M.S.A., Mahmoud, S.R. and Tounsi, A.

(2015), "A sinusoidal plate theory with 5-unknowns and stretching effect for thermomechanical bending of functionally graded sandwich plates", *Steel Compos. Struct.*, **18**(1), 235-253. https://doi.org/10.12989/scs.2015.18.1.235.

Hebali, H., Bakora, A., Tounsi, A. and Kaci, A. (2016), "A novel four variable refined plate theory for bending, buckling, and vibration of functionally graded plates", *Steel Compos. Struct.*, **22**(3), 473-495. https://doi.org/10.12989/scs.2016.22.3.473.

Hebali, H., Tounsi, A., Houari, M.S.A., Bessaim, A. and AddaBedia, E.A. (2014), "A new quasi-3D hyperbolic shear deformation theory for the static and free vibration analysis of functionally graded plates", *ASCE J. Eng. Mech.*, **140**(2), 374-383. https://doi.org/10.1061/(ASCE)EM.1943-7889.0000665.

Hellal, H., Bourada, M., Hebali, H., Bourada, F., Tounsi, A., Bousahla, A.A. and Mahmoud, S.R. (2019), "Dynamic and stability analysis of functionally graded material sandwich plates in hygro-thermal environment using a simple higher shear deformation theory", *J. Sandw. Struct. Mater.*, 1099636219845841. https://doi.org/10.1177/1099636219845841.

Houari, M.S.A., Tounsi, A. and Anwar Bég, O. (2013), "Thermoelastic bending analysis of functionally graded sandwich plates using a new higher order shear and normal deformation theory", *Int. J. Mech. Sci.*, **76**, 102-111. https://doi.org/10.1016/j.ijmecsci.2013.09.004.

Houari, M.S.A., Tounsi, A., Bessaim, A. and Mahmoud, S.R. (2016), "A new simple three-unknown sinusoidal shear deformation theory for functionally graded plates", *Steel Compos. Struct.*, **22**(2), 257-276. https://doi.org/10.12989/scs.2016.22.2.257.

Hsu, M.H. (2010), "Vibration analysis of orthotropic rectangular plates on elastic foundations", *Compos. Struct.*, **92**, 844-852. https://doi.org/10.1016/j.compstruct.2009.09.015.

https://doi.org/10.4028/www.scientific.net/JNanoR.54.1.

Hussain, M. and Naeem, M.N. (2019), "Rotating response on the vibrations of functionally graded zigzag and chiral single walled carbon nanotubes", *Appl. Math. Model.*, **75**, 506-520. https://doi.org/10.1016/j.apm.2019.05.039.

Hussain, M., Naeem, M.N., Tounsi, A. and Taj, M. (2019), "Nonlocal effect on the vibration of armchair and zigzag SWCNTs with bending rigidity", *Adv. Nano Res.* (Accepted)

Jha, D., Kant, T. and Singh, R. (2013), "Free vibration response of functionally graded thick plates with shear and normal deformations effects", *Compos. Struct.*, **96**, 799-823. https://doi.org/10.1016/j.compstruct.2012.09.034.

Jin, G., Su, Z., Shi, S., Ye, T. and Gao, S. (2014), "Three-dimensional exact solution for the free vibration of arbitrarily thick functionally graded rectangular plates with general boundary conditions", *Compos. Struct.*, **108**, 565-577. https://doi.org/10.1016/j.compstruct.2013.09.051.

Kaci, A., Houari, M.S.A., Bousahla, A.A., Tounsi, A. and Mahmoud, S.R. (2018), "Post-buckling analysis of shear-deformable composite beams using a novel simple two-unknown beam theory", *Struct. Eng. Mech.*, **65**(5), 621-631. https://doi.org/10.12989/sem.2018.65.5.621.

Kadari, B., Bessaim, A., Tounsi, A., Heireche, H., Bousahla, A.A. and Houari, M.S.A. (2018), "Buckling analysis of orthotropic nanoscale plates resting on elastic foundations", *J. Nano Res.*, **55**, 42-56. https://doi.org/10.4028/www.scientific.net/JNanoR.55.42.

Kar, V.R., Mahapatra, T.R. and Panda, S.K. (2017), "Effect of different temperature load on thermal post buckling behaviour of functionally graded shallow curved shell panels", *Compos. Struct.*, **160**, 1236-1247. https://doi.org/10.1016/j.compstruct.2016.10.125.

Karama, M., Harb, B.A., Mistou, S. and Caperaa, S. (1998), "Bending, buckling and free vibration of laminated composite with a transverse shear stress continuity model", *Compos. Part B*, **29**, 223-234. https://doi.org/10.1016/S1359-8368(97)00024-3.

Karami, B., Janghorban, M. and Tounsi, A. (2017), "Effects of triaxial magnetic field on the anisotropic nanoplates", *Steel Compos. Struct.*, **25**(3), 361-374. https://doi.org/10.12989/scs.2017.25.3.361.

Karami, B., Janghorban, M. and Tounsi, A. (2018a), "Galerkin's approach for buckling analysis of functionally graded anisotropic nanoplates/different boundary conditions", *Eng. Comput.*, **35**(4), 1297-1316. https://doi.org/10.1007/s00366-018-0664-9.

Karami, B., Janghorban, M. and Tounsi, A. (2018d), "Variational approach for wave dispersion in anisotropic doubly-curved nanoshells based on a new nonlocal strain gradient higher order shell theory", *Thin Wall. Struct.*, **129**, 251-264. https://doi.org/10.1016/j.tws.2018.02.025.

Karami, B., Janghorban, M. and Tounsi, A. (2018f), "Nonlocal strain gradient 3D elasticity theory for anisotropic spherical nanoparticles", *Steel Compos. Struct.*, **27**(2), 201-216. https://doi.org/10.12989/scs.2018.27.2.201.

Karami, B., Janghorban, M. and Tounsi, A. (2019a), "Wave propagation of functionally graded anisotropic nanoplates resting on Winkler-Pasternak foundation", *Struct. Eng. Mech.*, **7**(1), 55-66. https://doi.org/10.12989/sem.2019.70.1.055.

Karami, B., Janghorban, M. and Tounsi, A. (2019c), "On exact wave propagation analysis of triclinic material using three dimensional bi-Helmholtz gradient plate model", *Struct. Eng. Mech.*, **69**(5), 487-497. https://doi.org/10.12989/sem.2019.69.5.487.

Karami, B., Janghorban, M., Shahsavari, D. and Tounsi, A. (2018e), "A size-dependent quasi-3D model for wave dispersion analysis of FG nanoplates", *Steel Compos. Struct.*, **28**(1), 99-110. https://doi.org/10.12989/scs.2018.28.1.099.

Karami, B., Shahsavari, D. and Janghorban, M. (2018b), "Wave propagation analysis in functionally graded (FG) nanoplates under in-plane magnetic field based on nonlocal strain gradient theory and four variable refined plate theory", *Mech. Adv. Mat. Struct.*, **25**(12), 1047-1057. https://doi.org/10.1080/15376494.2017.1323143.

Karami, B., Shahsavari, D., Janghorban, M. and Tounsi, A. (2019b), "Resonance behavior of functionally graded polymer composite nanoplates reinforced with grapheme nanoplatelets", *Int. J. Mech. Sci.*, **156**, 94-105. https://doi.org/10.1016/j.ijmecsci.2019.03.036.

Karami, B., Shahsavari, D., Nazemosadat, S.M.R., Li, L. and Ebrahimi, A. (2018c), "Thermal buckling of smart porous functionally graded nanobeam rested on Kerr foundation", *Steel Compos. Struct.*, **29**(3), 349-362. https://doi.org/10.12989/scs.2018.29.3.349.

Khetir, H., Bachir Bouiadjra, M., Houari, M.S.A., Tounsi, A. and Mahmoud, S.R. (2017), "A new nonlocal trigonometric shear deformation theory for thermal buckling analysis of embedded nanosize FG plates", *Struct. Eng. Mech.*, **64**(4), 391-402. https://doi.org/10.12989/sem.2017.64.4.391.

Khiloun, M., Bousahla, A.A., Kaci, A., Bessaim, A., Tounsi, A. and Mahmoud, S.R. (2019), "Analytical modeling of bending and vibration of thick advanced composite plates using a four-variable quasi 3D HSDT", *Eng. Comput.*, 1-15. https://doi.org/10.1007/s00366-019-00732-1.

Klouche, F., Darcherif, L., Sekkal, M., Tounsi, A. and Mahmoud, S.R. (2017), "An original single variable shear deformation theory for buckling analysis of thick isotropic plates", *Struct. Eng. Mech.*, **63**(4), 439-446. https://doi.org/10.12989/sem.2017.63.4.439.

Kneifati, M.C. (1985), "Analysis of plates on a Kerr foundation model", *J. Eng. Mech.*, **111**, 1325-1342. https://doi.org/10.1061/(ASCE)0733-9399(1985)111:11(1325).

Kolahchi, R., Safari, M. and Esmailpour, M. (2016), "Dynamic stability analysis of temperature-dependent functionally graded CNT-reinforced visco-plates resting on orthotropic elastomeric medium", *Compos. Struct.*,**150**, 255-265. https://doi.org/10.1016/j.compstruct.2016.05.023.

Larbi Chaht, F., Kaci, A., Houari, M.S.A., Tounsi, A., Anwar Bég, O. and Mahmoud, S.R. (2015), "Bending and buckling analyses of functionally graded material (FGM) size-dependent nanoscale beams including the thickness stretching effect", *Steel. Compos. Struct.*, **18**(2), 425-442. https://doi.org/10.12989/scs.2015.18.2.425.

Li, J.F., Takagi, K., Ono, M., Pan, W., Watanabe, R., Almajid, A. and Taya, M. (2003), "Fabrication and evaluation of porous piezoelectric ceramics and porosity-graded piezoelectric actuators", *J. Am. Ceram. Soc.*, **86**, 1094-1098. https://doi.org/10.1111/j.1151-2916.2003.tb03430.x.

Loh, E.W.K. and Deepak, T.J. (2018), "Structural insulated panels: State-of-the-art", *Trend. Civil Eng. Arch.*, **3**(1) 336-340. https://doi.org/10.32474/TCEIA.2018.03.000151.

Lü, C., Lim, C.W. and Chen, W. (2009), "Exact solutions for free vibrations of functionally graded thick plates on elastic foundations", *Mech. Adv. Mater. Struct.*, **16**, 576-584. https://doi.org/10.1080/15376490903138888.

Mahi, A., Adda Bedia, E.A. and Tounsi, A. (2015), "A new hyperbolic shear deformation theory for bending and free vibration analysis of isotropic, functionally graded, sandwich and laminated composite plates", *Appl. Math. Model.*, **39**(9), 2489-2508. https://doi.org/10.1016/j.apm.2014.10.045.

Mantari, J., Granados, E., Hinostroza, M. and Soares, C.G. (2014), "Modelling advanced composite plates resting on elastic foundation by using a quasi-3D hybrid type HSDT", *Compos. Struct.*, **118**, 455-471. https://doi.org/10.1016/j.compstruct.2014.07.039.

Medani, M., Benahmed, A., Zidour, M., Heireche, H., Tounsi, A., Bousahla, A.A., Tounsi, A. and Mahmoud, S.R. (2019), "Static and dynamic behavior of (FG-CNT) reinforced porous sandwich plate", *Steel Compos. Struct.*, **32**(5), 595-610. https://doi.org/10.12989/scs.2019.32.5.595.

Meksi, R, Benyoucef, S., Mahmoudi, A., Tounsi, A., Adda Bedia, E.A. and Mahmoud, SR. (2019), "An analytical solution for bending, buckling and vibration responses of FGM sandwich plates", *J. Sandw. Struct. Mater.*, **21**(2), 727-757. https://doi.org/10.1177/1099636217698443.

Menasria, A., Bouhadra, A., Tounsi, A., Bousahla, A.A. and Mahmoud, S. (2017), ''A new and simple HSDT for thermal stability analysis of FG sandwich plates'', *Steel Compos. Struct.*, **25**(2), 157-175. https://doi.org/10.12989/scs.2017.25.2.157.

Merdaci, S., Tounsi, A. and Bakora, A. (2016), "A novel four variable refined plate theory for laminated composite plates", *Steel Compos. Struct.*, **22**(4), 713-732. https://doi.org/10.12989/scs.2016.22.4.713.

Meziane, M.A.A., Abdelaziz, H.H. and Tounsi, A. (2014), "An efficient and simple refined theory for buckling and free vibration of exponentially graded sandwich plates under various boundary conditions", *J. Sandw. Struct. Mater.*, **16**(3), 293-318. https://doi.org/10.1177/1099636214526852.

Mokhtar, Y., Heireche, H., Bousahla, A.A., Houari, M.S.A., Tounsi, A. and Mahmoud, S. (2018), ''A novel shear deformation theory for buckling analysis of single layer graphene sheet based on nonlocal elasticity theory'', *Smart Struct. Syst.*, **21**(4), 397-405. https://doi.org/10.12989/sss.2018.21.4.397.

Mouffoki, A., Adda Bedia, E.A., Houari, M.S.A., Tounsi, A. and Mahmoud, S.R. (2017), "Vibration analysis of nonlocal advanced nanobeams in hygro-thermal environment using a new two-unknown trigonometric shear deformation beam theory", *Smart Struct. Syst.*, **20**(3), 369-383. https://doi.org/10.12989/sss.2017.20.3.369.

Naebe, M. and Shirvanimoghaddam, K. (2016), "Functionally graded materials: a review of fabrication and properties", *Appl. Mater. Today*, **5**, 223-245. https://doi.org/10.1016/j.apmt.2016.10.001.

Pasternak, P. (1954), "On a new method of analysis of an elastic foundation by means of two foundation constants", *Gosudarstvennoe Izdatelstvo Literaturipo Stroitelstvu i Arkhitekture*, Moscow.

Rad, A.B., Farzan-Rad, M.R. and Majd, K.M. (2017), "Static analysis of non-uniform heterogeneous circular plate with porous material resting on a gradient hybrid foundation involving friction force", *Struct. Eng. Mech.*, **64**(5), 591-610. https://doi.org/10.12989/sem.2017.64.5.591.

Rajabi, J. and Mohammadimehr, M. (2019), "Bending analysis of a micro sandwich skew plate using extended Kantorovich method based on Eshelby-Mori-Tanaka approach", *Comput. Concrete*, **23**(5), 361-376. https://doi.org/10.12989/cac.2019.23.5.361.

Sekkal, M., Fahsi, B., Tounsi, A. and Mahmoud, S.R. (2017a), "A novel and simple higher order shear deformation theory for stability and vibration of functionally graded sandwich plate", *Steel Compos. Struct.*, **25**(4), 389-401. https://doi.org/10.12989/scs.2017.25.4.389.

Sekkal, M., Fahsi, B., Tounsi, A. and Mahmoud, S.R. (2017b), "A new quasi-3D HSDT for buckling and vibration of FG plate", *Struct. Eng. Mech.*, **64**(6), 737-749. https://doi.org/10.12989/sem.2017.64.6.737.

Selmi, A. and Bisharat, A. (2018), "Free vibration of functionally graded SWNT reinforced aluminum alloy beam", *J. Vibroeng.*, **20**(5), 2151-2164. https://doi.org/10.21595/jve.2018.19445.

Shahadat, M.R.B., Alam, M.F., Mandal, M.N.A and Ali, M.M. (2018), "Thermal transportation behaviour prediction of defective graphene sheet at various temperature: A Molecular Dynamics Study", *Am. J. Nanomater.*, **6**(1), 34-40. https://doi.org/10.12691/ajn-6-1-4.

Shahsavari, D. and Janghorban, M. (2017), "Bending and shearing responses for dynamic analysis of single-layer graphene sheets under moving load", *J. Brazil. Soc. Mech. Sci. Eng.*, **39**(10), 3849-3861. https://doi.org/10.1007/s40430-017-0863-0.

Shahsavari, D., Karami, B. and Mansouri, S. (2018a), "Shear buckling of single layer graphene sheets in hygrothermal environment resting on elastic foundation based on different nonlocal strain gradient theories", *Eur. J. Mech. A, Solid.*, **67**, 200-214. https://doi.org/10.1016/j.euromechsol.2017.09.004.

Shahsavari, D., Shahsavari, M., Li, L. and Karami, B. (2018b), "A novel quasi-3D hyperbolic theory for free vibration of FG plates with porosities resting on Winkler/Pasternak/Kerr foundation", *Aerosp. Sci. Technol.*, **72**, 134-149. https://doi.org/10.1016/j.ast.2017.11.004.

Shimpi, R. and Patel, H. (2006a), "Free vibrations of plate using two variable refined plate theory", *J. Sound Vib.*, **296**, 979-999. https://doi.org/10.1016/j.jsv.2006.03.030.

Shimpi, R. and Patel, H. (2006b), "A two variable refined plate theory for orthotropic plate analysis", *Int. J. Solid. Struct.*, **43**, 6783-6799. https://doi.org/10.1016/j.ijsolstr.2006.02.007.

Sobhy, M. (2013), "Buckling and free vibration of exponentially graded sandwich plates resting on elastic foundations under various boundary conditions", *Compos. Struct.*, **99**, 76-87. https://doi.org/10.1016/j.compstruct.2012.11.018.

Sofiyev, A.H. and Avcar, M. (2010), "The stability of cylindrical shells containing an FGM layer subjected to axial load on the Pasternak foundation", *Eng.*, **2**(4), 228. https://doi.org/10.4236/eng.2010.24033.

Thai, H.T. and Choi, D.H. (2011), "A refined plate theory for functionally graded plates resting on elastic foundation", *Compos. Sci. Technol*., **71**, 1850-1858. https://doi.org/10.1016/j.compscitech.2011.08.016.

Thai, H.T. and Kim, S.E. (2012), "Analytical solution of a two variable refined plate theory for bending analysis of orthotropic Levy-type plates", *Int. J. Mech. Sci*., **54**, 269-276. https://doi.org/10.1016/j.ijmecsci.2011.11.007.

Thai, H.T. and Kim, S.E. (2013), "A simple quasi-3D sinusoidal shear deformation theory for functionally graded plates", *Compos. Struct*., **99**, 172-180. https://doi.org/10.1016/j.compstruct.2012.11.030.

Thai, H.T. and Kim, S.E. (2015), "A review of theories for the modeling and analysis of functionally graded plates and shells", *Compos. Struct*., **128**, 70-86. https://doi.org/10.1016/j.compstruct.2015.03.010.

Thai, H.T., Vo, T., Bui, T. and Nguyen, T.K. (2014), "A quasi-3D hyperbolic shear deformation theory for functionally graded plates", *Acta Mech*., **225**, 951-964. https://doi.org/10.1007/s00707-013-0994-z.

Tounsi, A., Ait Atmane, H., Khiloun, M., Sekkal, M., Taleb, O. and Bousahla, A.A. (2019), "On buckling behavior of thick advanced composite sandwich plates", *Compos. Mater. Eng.*, **1**(1), 1-19.

Tounsi, A., Houari, M.S.A., Benyoucef, S. and AddaBedia, E.A. (2013), "A refined trigonometric shear deformation theory for thermoelastic bending of functionally graded sandwich plates", *Aerosp. Sci. Tech*., **24**, 209-220. https://doi.org/10.1016/j.ast.2011.11.009.

Wang, Y., Tham, L. and Cheung, Y. (2005), "Beams and plates on elastic foundations: a review", *Prog. Struct. Eng. Mater*., **7**, 174-182. https://doi.org/10.1002/pse.202.

Wattanasakulpong, N. and Ungbhakorn, V. (2014), "Linear and nonlinear vibration analysis of elastically restrained ends FGM beams with porosities", *Aerosp. Sci. Technol*., **32**(1), 111-120. https://doi.org/10.1016/j.ast.2013.12.002.

Winkler, E. (1867), "Die lehre von der elastizität und festigkeit (The Theory of Elasticity and Stiffness)", H. Dominicus, Prague, Czechoslovakia.

Yahia, S.A, Ait Atmane, H., Houari, M.S.A. and Tounsi, A. (2015), "Wave propagation in functionally graded plates with porosities using various higher-order shear deformation plate theories", *Struct. Eng. Mech*., **53**(6), 1143-1165. http://dx.doi.org/10.12989/sem.2015.53.6.1143.

Yazid, M., Heireche, H., Tounsi, A., Bousahla, A.A. and Houari, M.S.A. (2018), "A novel nonlocal refined plate theory for stability response of orthotropic single-layer graphene sheet resting on elastic medium", *Smart Struct. Syst*., **21**(1), 15-25. https://doi.org/10.12989/sss.2018.21.1.015.

Yeghnem, R., Guerroudj, H.Z., Amar, LHH., Meftah, S.A., Benyoucef, S., Tounsi, A. and Adda Bedia, E.A. (2017), "Numerical modeling of the aging effects of RC shear walls strengthened by CFRP plates: A comparison of results from different "code type" models", *Comput. Concrete*, **19**(5), 579-588. https://doi.org/10.12989/cac.2017.19.5.579.

Youcef, D.O., Kaci, A., Benzair, A., Bousahla, A.A. and Tounsi, A. (2018), "Dynamic analysis of nanoscale beams including surface stress effects", *Smart Struct. Syst*., **21**(1), 65-74. https://doi.org/10.12989/sss.2018.21.1.065.

Younsi, A., Tounsi, A., Zaoui, F.Z., Bousahla, A.A. and Mahmoud, S. (2018), "Novel quasi-3D and 2D shear deformation theories for bending and free vibration analysis of FGM plates", *Geomech. Eng.*, **14**(6), 519-532. https://doi.org/10.12989/gae.2018.14.6.519.

Zaoui, F.Z., Ouinas, D. and Tounsi, A. (2019), "New 2D and quasi-3D shear deformation theories for free vibration of functionally graded plates on elastic foundations", *Compos. Part B*, **159**, 231-247. https://doi.org/10.1016/j.compositesb.2018.09.051.

Zarga, D., Tounsi, A., Bousahla, A.A., Bourada, F. and Mahmoud, S.R. (2019), "Thermomechanical bending study for functionally graded sandwich plates using a simple quasi-3D shear deformation theory", *Steel Compos. Struct.*, **32**(3), 389-410. https://doi.org/10.12989/scs.2019.32.3.389.

Zemri, A., Houari, M.S.A., Bousahla, A.A. and Tounsi, A. (2015), "A mechanical response of functionally graded nanoscale beam: an assessment of a refined nonlocal shear deformation theory beam theory", *Struct. Eng. Mech*., **54**(4), 693-710. https://doi.org/10.12989/sem.2015.54.4.693.

Zhou, D., Cheung, Y., Au, F. and Lo, S. (2002), "Three-dimensional vibration analysis of thick rectangular plates using Chebyshev polynomial and Ritz method", *Int. J. Solid. Struct*., **39**, 6339-6353. https://doi.org/10.1016/S0020-7683(02)00460-2.

Zhu, J., Lai, Z., Yin, Z., Jeon, J. and Lee, S. (2001), "Fabrication of ZrO2-NiCr functionally graded material by powder metallurgy", *Mater. Chem. Phys*., **68**(1-3), 130-135. https://doi.org/10.1016/S0254-0584(00)00355-2.

Zidi, M., Houari, M.S.A., Tounsi, A., Bessaim, A. and Mahmoud, S.R. (2017), "A novel simple two-unknown hyperbolic shear deformation theory for functionally graded beams", *Struct. Eng. Mech*., **64**(2), 145-153. https://doi.org/10.12989/sem.2017.64.2.145.

Zidi, M., Tounsi, A., Houari, M.S.A. and Bég, O.A. (2014), "Bending analysis of FGM plates under hygro-thermo-mechanical loading using a four variable refined plate theory", *Aerosp. Sci. Tech*., **34**, 24-34. https://doi.org/10.1016/j.ast.2014.02.001.

Zine, A., Tounsi, A., Draiche, K., Sekkal, M. and Mahmoud, S.R. (2018), "A novel higher-order shear deformation theory for bending and free vibration analysis of isotropic and multilayered plates and shells", *Steel Compos. Struct.*, **26**(2), 125-137. https://doi.org/10.12989/scs.2018.26.2.125.

CC